TNO Built Environment and Geosciences

Princetonlaan 6
P.O. Box 80015
3508 TA Utrecht
The Netherlands

www.tno.nl

T +31 30 256 42 56
F +31 30 256 44 75
info-BenO@tno.nl

TNO report

TNO-034-UT-2009-01569

Terschelling Basin and southern Dutch Central Graben Mapping and modeling – Area 2A

Date	1 August 2009
Author(s)	J.M. Verweij N. Witmans
Assignor	
Project number	034.20780 NCP-2A

Classification report
Title
Abstract
Report text
Appendices

Number of pages	65
Number of appendices	14

Conclusions and management summary

To serve future and current operators in the oil industry and governmental and non-governmental organisations a comprehensive subsurface model of the Dutch offshore is being generated. The Netherlands Continental Shelf area is divided into seven sub-areas that represent more or less structural entities during Late Jurassic to Early Cretaceous time. In this report the results of sub-area NCP-2A, including the Terschelling Basin and the southern part of the Dutch Central Graben, are described.

The basin boundary fault zones of the Terschelling Basin and the southern part of the Dutch Central Graben in combination with the fault-associated salt structures form the structural framework of the area. Structural grid shows a dominance of two directions: NNE-SSW and WNW-ESE. Different phases of fault activation and reactivation were identified and Zechstein salt movements appear to have played a crucial rule in compartmentalisation of the basins during periods of intensified tectonics. Sedimentary facies distribution, thickness and erosion of the Paleozoic–Cenozoic stratigraphic units are strongly related to the complex structural evolution of the area.
The detailed mapping and assessment of rock and fluid properties (reservoir porosities, pressures, salinities, temperatures, source rock maturity, characteristics of oil and gas) presented herein are essential data for future and current petroleum geological and prospect evaluation.

Analysis and interpretation of the rock and fluid properties provide additional important information for evaluation of petroleum systems. The pressure data revealed that the salt dominated study area is highly overpressured. Characterisation of pressure compartments includes the identification of regional seals as well as local leakage zones. The temperature distribution indicates large lateral variations related to the many salt structures of relatively high thermal conductivity.

The report shows that next to the main source rocks for gas, i.e. the coal measures of the Limburg Group, coal layers in the Central Graben Subgroup (Upper Jurassic Schieland Group) are considered to be a potential secondary gas source. The Posidonia Shale Formation is the main source rock for oil and potential new source horizons occur in the Aalburg and Sleen Formations of the Altena Group. Next to proven Permian, Triassic und Upper Jurassic reservoirs in the study area, other potential reservoirs, for example in the Upper Carboniferous Hospital Ground and Step Graben formations, the Upper Cretaceous Chalk Group and Quaternary sand offer an excellent opportunity to operators for further exploration.

Contents

1 Introduction

1.1 Mapping of the deep subsurface of the Netherlands offshore (NCP-2 project)

The detailed mapping of seven offshore areas on the Netherlands Continental Shelf was initiated in late 2005 and will be finalised in 2010. It builds on and goes one step beyond the previous regional mapping of the Netherlands onshore and offshore. In 2004 the publication of the Geological Atlas of the Subsurface of the Netherlands – *onshore* rounded off the onshore regional mapping project and a 'quick and dirty' offshore mapping (NCP-1 project) was completed in 2006 (viz. http://www.nlog.nl; Duin et al. 2006).

The main aim of the detailed mapping of seven sub-areas is to present a more comprehensive model of the subsurface to future and current operators in the oil industry and to governmental and non-governmental organisations for, amongst other things, the spatial planning of the Dutch subsurface. The deliverables include:
3D geological framework (depth and thickness grids)
Rock and fluid parameters (petrophysical parameters, P, T, Vr)
3D burial histories
Petroleum system analysis
All deliverables, such as maps, grids and graphs, can be downloaded at the http://www.nlog.nl site. When applicable, regular updates will be made available on the site.

1.2 Definition of mapping areas

Based on consultation with the exploration departments of the oil companies operating in the Netherlands it was decided to divide the offshore area into seven sub-areas (fig. 1). These areas represent more or less structural entities during Late Jurassic to Early Cretaceous. (fig. 2). The detailed mapping project started with sub-area NCP-2A: Terschelling Basin and the southern part of the Dutch Central Graben (fig. 2).

1.3 Detailed mapping of the Terschelling Basin and the southern part of the Dutch Central Graben

The detailed mapping was focussed on the assessment of the present-day stratigraphic and structural framework of the sedimentary fill of the area as well as on the properties of rocks and fluids it contains, such as reservoir porosities, pressures, salinities, source rock maturity, characteristics of oil and gas. Special attention was paid to improve the lithostratigraphic sub-division of the complex Upper Jurassic sequence, and to provide new porosity data for the main reservoir units in the Upper Rotliegend Group, Germanic Trias groups and the Schieland Group. In addition 3D basin modelingwas used to integrate the data, visualise the geodynamic, geothermal and geofluid history the area and as such to provide additional information for evaluating the petroleum systems.
This report concerns the present-day setting and characteristics of the study area.

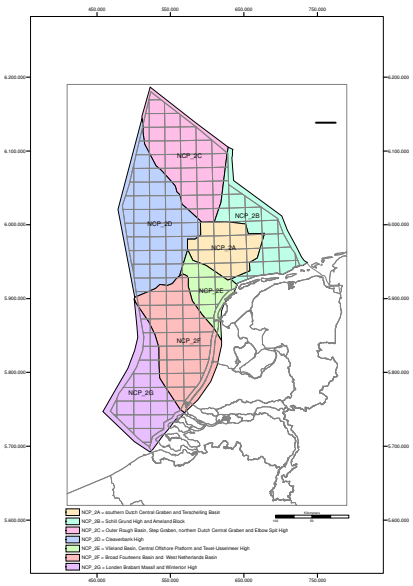

Figure 1.1 NCP-2 areas; Location of the project area NCP-2A: Terschelling Basin and the southern part of the Dutch Central Graben

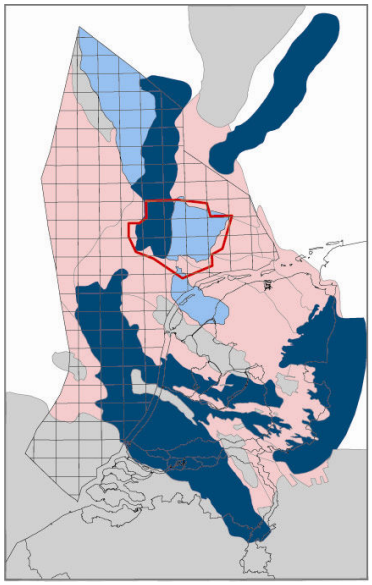

Figure 1.2 Structural setting at Late Jurassic-Early Cretaceous.
Grey: highs, Pink: platforms, Dark blue: basins with Lower Jurassic, Light blue: basins without Lower Jurassic

2 Database

Most data used in the project are publicly released seismic surveys and borehole data that were acquired by various oil companies. In addition we used published information, research results and laboratory analyses from previous in-house studies. Also reports from third parties on boreholes or regional studies were consulted.

2.1 Stratigraphic data/Dino database

The basic information for the mapping project was derived from the released data of 80 boreholes available in the DINO database (see Appendix 1). The selection criteria for these boreholes include: the presence of a specific stratigraphic interval of interest, the presence of complete stratigraphic intervals, the total depth of the borehole, geographic spacing, the presence of hydrocarbons, the availability of a representative set of well logs, the availability of cores in stratigraphic intervals of interest. At the start of the project stratigraphic information in the DINO database varied both in quality and in detail.

2.2 Seismic data

The available regional seismic framework for the entire offshore area was used as the groundwork for the detailed mapping using released 3D seismic surveys (Appendix 2) No additional 2D surveys were used in the project. The inlines of most surveys have an E-W orientation and intersect the dominant geological structures at high angles. The quality of the seismic signal is generally good to fair from the ground surface to the Top Zechstein horizon, enabling a reliable interpretation for this interval. Below the Zechstein Group the quality of the signal is mostly too poor to allow a reliable regional interpretation. Mapping the deeper levels depended on available well data.

In general, every 10^{th} inline and every 25^{th} xline was interpreted for each seismic survey. In structurally less complicated areas a wider spaced grid consisting of every 20^{th} inline and every 50^{th} xline, was sufficient to map the surfaces with a level of accuracy.

2.3 Borehole data

2.3.1 Well logs

The available well logs for the selected 80 wells include gamma-ray, sonic and occasionally also neutron-density logs.

2.3.2 Temperature measurements

Approximately 600 quality-controlled temperature data from 51 oil and gas wells in the study area were available for analysis. This temperature database includes data from different sources, such as bottom hole temperatures, Horner-extrapolated temperatures, along-hole measured temperatures, and temperatures observed during drill stem tests and repeat formation tests. There are large differences in reliability of these temperature data. Most temperatures were measured at depths of more than 1500 m. These data mainly represent temperature measurements in sediments of Triassic to Cretaceous age.

2.3.3 Well test data

The pressure measurements from wireline formation tests (RFT tests) and leak-off tests carried out in approximately 30 wells were used to characterise the pressure and fluid flow system in the Terschelling Basin and the southern part of the Dutch Central Graben.

2.3.4 Fluid properties

Composition oil and gas

The characterisation of the natural oil and gas in the Terschelling Basin and the southern Dutch Central Graben is based on analyses and interpretations from stranded fields presented in the non-confidential (the databases are publicly accessible on www.nlog.nl). The non-confidential database on the composition of natural gas contains approximately 90 analyses of gas samples from 30 wells in the study area, while 19 analyses also include information on the isotopic compositions of hydrocarbons, nitrogen and/or carbon dioxide.

2.3.5 Cores and cuttings

In 33 wells within the area core measurements were available for petrophysical analyses. If necessary we used additional measurements on cores from wells bordering the area (TNO report 2007). For the sedimentological study of the Upper Jurassic sediments new core descriptions were made for 11 wells (TNO report 2007). Furthermore, cuttings of more than 20 wells were analysed for biostratigraphic studies of Tertiary, Upper Jurassic and Carboniferous rocks.
New organic geochemical and organic-petrological information was derived from measurements on 67 samples selected from 22 wells (the analysis results are incorporated in the DINO database).

2.4 Information from literature

Apart from the references listed under chapter 5, consultancy reports and reports from operators concerning the wells or the area were used for reference. These reports contain information about the geological and stratigraphic subdivision, biostratigraphy, coe descriptions and analyses, geochemical data, pressure and temperature data.

3 Approach

The basic methods used in the mapping process include lithostratigraphic (re)-interpretation of well logs, incorporation of the lithostratigraphic information into the seismic interpretation, time-to-depth conversion of the seismic velocity and the construction of depth and thickness maps of the eight major lithostratigraphic units. Additional units of importance for the petroleum system were identified by lithostratigraphic well correlation (reservoir and source rock units). Biostratigraphic and sedimentological analyses were applied to improve the lithostratigraphic sub-division of the Upper Jurassic. Petrophysical analysis provided new porosity data for the main reservoir units, hydrodynamic analysis resulted in the characterisation of the pressure and fluid flow system, and maturity analysis on samples increased the knowledge on the present-day source rock maturities.1D, 2D and 3D basin modelingof the entire study area was used to highlight the relation between the burial history of the basin and the petroleum play, including the temperature and maturation history of its source rocks, timing of hydrocarbon generation, migration and formation of traps.

3.1 Construction 3D geological model

3.1.1 Well log correlation

The gamma-ray, sonic and, if available the neutron-density, logs were combined into a digital composite well log for each of the selected 80 wells. The composite logs of all 80 wells were loaded into the Petrel programme and lithostratigraphically (re-) interpreted on member level. The construction of 10 to 12 cross sections, some on group level, allowed a detailed lithostratigraphic interpretation. Additional cross-sections were set up with a good spatial distribution to create a more regional view. The interpretation of the composite well logs resulted in a more detailed lithostratigraphic subdivision of the area. The new detailed stratigraphic information at well locations was incorporated in the interpretation of the seismic data. At a later stage of the project, the thicknesses of the main reservoir units that were identified at well level were implemented in the grids of the 3D-depth model.

3.1.2 Biostratigraphic analysis of the Upper Jurassic

The ‘Upper-Jurassic’ sequence was biostratigraphically interpreted in 20 selected wells, and subsequently placed in a tectono-stratigraphic framework following the approach of Abbink et al. (2006). The approach involved the correlation of about 50 wells with or without biostratigraphic data of the Upper Jurassic sediments. A sedimentological study was carried out simultaneously and provided a depositional environment for the Upper Jurassic sediments. The combined result of the biostratigrahic and the sedimentologic studies will lead to a new lithostratigraphic subdivision of the Upper Jurassic at the end of this mapping project in 2010 (Annex F).

3.1.3 Sedimentological analysis of the Upper Jurassic

A profound sedimentological study was performed on the B2 sequence of the Upper Jurassic, which correlates with tectono-sequence 2 in the tectono-sequence framework of Abbink et al. (2006). Core descriptions, biostratigraphical data and well logs were used to establish a facies distribution in the Terschelling Basin and the southern Dutch Central Graben (Stegers, 2006). The work performed in this study contained core descriptions, correlation of the cores to the well logs, tying the wells into the seismic sections and the construction of paleogeographic maps. New core descriptions were made at 11 well locations.

Subsequently 4 correlation panels were set up and the depositional environments were identified in the wells based on the combined interpretation of the core descriptions, cuttings description and biostratigraphic data. Using seismic sections parallel to the correlation panels allowed to re-construct the geometry of the depositional and stratigraphic units. The results can be downloaded from the nlog site.

3.1.4 Seismic interpretation

The stratigraphic interpretation of the 3D seismic surveys was focussed on identification of the lower boundaries of the Upper North Sea Group, Lower North Sea Group, Chalk Group, Rijnland Group, Schieland Group, Altena Group, Upper and Lower Germanic Trias groups and the Zechstein Group. In addition, the base of the intra-Upper Jurassic marker B3, which is the base of tectono-sequence 3 Abbink et al. (2006) was seismically interpreted. This marker forms the base of the Scruff Group.

No separate reservoir units were seismically interpreted due to their limited thickness and/or distribution.

For constructing the structural model the interpretation was focussed on identifying the major faults i.e. faults with large (vertical) offsets and faults that are important for the definition of the structural elements. The faults were labelled according to the lithostratigraphic groups which they offset, because such information is a prerequisite for the construction of the 3D model. The lithostratigraphic interpretations of wells were converted to the time domain using available check shot data, and used to support the seismic interpretation.

3.1.5 3D time model

For the 3D-modelingand the time-depth conversion the program Petrel, version 2005, was used. The horizon and fault interpretations formed the base to construct the 3D-time model. The fault interpretations were converted to fault pillars, which were edited to fit the fault planes into the horizon interpretations.
The study area is characterised by numerous salt structures. The faults above and below those structures are decoupled and are treated as two independent fault systems in this model.

In Petrel the modeled fault planes run throughout the entire model, which consequently can lead to crossing fault planes. Petrel uses the fault pillars to construct the 3D-time model, which is the main input for the time-depth conversion, in which those crossing faults are not allowed. Therefore, one model was constructed for the faults displacing the base Zechstein and a second model with the faults not displacing the Zechstein as a result of salt movement.
A complication in this work flow is that at many places the salt is completely absent as a result of salt movement. In these areas the faults also displace the Triassic deposits and for this reason a third model was created.
Another complication is the presence of lateral Zechstein salt intrusions into the Upper Triassic. Because of the deviating velocity a fourth 3D-model was created in areas with these intrusions.

Time-depth conversion

The interpreted seismic data were converted from time to depth using a slightly modified version of the seismic velocity model of Van Dalfsen, e*t al*. (2007). This model consists of V_0-grids and a constant k for all groups except for the Zechstein, for which a V_{int}-grid was created based on borehole information from the entire Dutch on- and offshore. There are no velocity data available for the salt intrusions and therefore a constant halite velocity of 4450 m/s was assumed.
The resulting depth surfaces corresponding to the bases of the nine stratigraphic (sub-)groups were fitted together and if needed, slightly edited to form the 3D-depth model.

3.2 Assessment rock and fluid properties and conditions

3.2.1 Petrophysical analysis

The analysis of petrophysical parameters focussed on obtaining porosity data for several reservoir-type rocks in this area, including reservoir units in the Schieland Group, the Lower Detfurth and Volpriehausen Sandstone Members of the Lower Germanic Triassic Group and the Upper Rotliegend Slochteren Formation (Benedictus, 2007).

For this purpose bulk density and, to a lesser extent, neutron logs were used to estimate porosities. There exists a simple theoretical relationship between porosity and bulk density that also involves grain density and pore-fluid density. Grain density data were obtained from core-sample measurements resulting in representative mean values for the individual lithostratigraphic units (see Annex J). The pore-fluid recorded by the logging tool mainly consists of mud filtrate that invaded the porous rock. Consequently, estimates on pore-fluid density are well constrained using measured resistance of the mud filtrate, which is directly related to the salinity and therefore to the density of the mud filtrate.

However, in gas-bearing zones the mud filtrate is pushed out by gas, causing the logging tool to record a signal that is affected by the presence of gas in the pore space. In order to correct for this effect the arithmetic mean of the calculated porosity and the neutron log derived porosity was used as the best porosity estimate. As the neutron log porosity represents default limestone porosity, the values are first corrected for sand-shale lithologies.

Interpretation of the gamma-ray logs was applied to assess the net-to-gross ratio of the reservoir units.

The mean net porosity and the net-to-gross ratio were calculated for reservoir units in 30 wells in the study area and 9 wells just outside the area. The results can be found in Annex J. The report can be downloaded from the nlog site.

3.2.2 Maturity analysis

Analyses of 67 samples selected from 22 wells provided new organic geochemical and organic petrological information on stratigraphic units containing organic matter (results are in the DINO database). The organic matter was characterised by – amongst other things - vitrinite reflectance, total organic carbon (TOC), and hydrogen index (HI). These parameters were used as calibration data for the basin modelling.

Vitrinite reflectance is an optical (microscopic) maturity parameter. Increasing vitrinite reflectance values are related to the progressive aromatisation of the kerogen with accompanying loss of hydrogen in the form of hydrocarbon gases with increasing time and temperature.
Vitrinite, a maceral derived from woody plant material, is common in coal and organic-rich shale. Vitrinite reflectance is a measure of the proportion of light reflected from a polished vitrinite grain. It is related to the degree of metamorphism of the vitrinite grain and can be related to other thermal maturity indicators. Since vitrinite changes predictably and consistently upon heating, its reflectance is a useful measurement of source rock maturity.

Sample preparation and vitrinite reflectance measurements were performed according to international standard methods (ISO 7404-2, 1985 and ISO 7404-5, 1994) by an accredited petrographer (ICCP). For each sample hundred readings are randomly performed on vitrinite particles to obtain a statistically acceptable population. However, for most of the samples the amount of suitable vitrinite particles was insufficient to measure the required hundred points, thereby reducing the accuracy of the measurement. The mean value of the readings per sample represents the vitrinite reflectance of the sample (%R_o or % R_{max}), the standard deviation indicates the uncertainty in the measurement.

The full procedure for the measurement of vitrinite reflectance values is given in the standard operating procedures GL-WV 201 (sample preparation organic petrology) and GL-WV 202 (vitrinite reflectance).

On the basis of the number of measurements and the standard deviation a statement can be made on the 'reliability' of the measurement. The criteria are given in the table below.

A	High reliability, (Stdv ≤ 0.05; N ≥ 40)
B	Average reliability, (0.05 ≤ Stdv ≥ 0.10; 15 ≤ N ≥ 40)
C	Low reliability, (Stdv ≥ 0.10; N ≤ 15)

In some cases two reflectance populations are recognised in the histogram. In such cases two additional histograms (including their statistics) of the two individual populations are given.

The results of the vitrinite reflectance measurements are presented by their statistics (average value, standard deviation and number of measurements per sample) and a label describing the reliability of the measurement is given. A summary of the results is given in Annex M.

3.2.3 Temperature analysis

In order to characterise the present-day thermal conditions in the Terschelling Basin and the southern part of the Dutch Central Graben we calculated and mapped geothermal gradients. A Bayesian statistical method was applied to calculate the geothermal gradient at each well, using all the temperature data and additional corrected bottom hole temperatures for that well, including standard deviations for the different types of temperature data, and assuming a surface temperature of 9^{o}C with a standard deviation of 2^{o}C.

3.2.4 Hydrodynamic analysis/characterisation

Multi-well plots of fluid pressure versus depth and leak-off pressures versus depth plots were used to characterise and visualise the present-day pressure distribution in different parts of the basin and in different reservoir units.

Excess fluid pressures were calculated in relation to density corrected hydrostatic pressures. The excess pressure or overpressure of formation water at a certain depth is the difference between the measured pore pressure and the hydrostatic pressure at that depth; the excess pressure of hydrocarbon fluids is the difference between the measured pressure of the oil or gas and the hydrostatic (water) pressure at that depth. The often applied standard hydrostatic gradient represents the increase of pressure with depth for formation water of constant seawater density (1020 mg/cm3). The density corrected hydrostatic gradient includes the effects of increasing salinity, and corresponding increasing density, with depth. Three geological cross-section with excess pressures were created to characterise the regional variation in pressure conditions in the study area.

Multi-well plots of fluid pressure versus depth and leak-off pressures versus depth plots were used to characterise and visualise the present-day pressure distribution in different parts of the basin and in different reservoir units.

3.2.5 Fluid composition analysis

Cross-plots of the carbon and hydrogen isotopic composition of methane were created to characterise the natural gases in the study area. To study the origin of the non-hydrocarbon components in the gas accumulations the isotopic composition of nitrogen and carbon dioxide were plotted against the nitrogen and carbon dioxide content, respectively. Selected characteristics of the natural oil and gas in the Terschelling Basin and the Dutch Central Graben were mapped to show the regional variation.

3.3 Construction 2D maps and cross-sections

The depth and thickness surfaces in Petrel are converted to 2D grids and imported into ArcGIS. Maps of the nine major stratigraphic units (Upper North Sea, Middle and Lower North Sea, Chalk, Rijnland, Schieland and Altena groups, Upper and Lower Germanic Trias subgroups and the Zechstein Group) are presented here. Also the depth and thickness of the Scruff Group based on seismic interpretation is added.

Additionally, the depth and thickness of the Upper Rotliegend Group was constructed from well data, as were the depth map of the Posidonia Shale Formation and thickness maps of the Terschelling Sandstone reservoir, the Lower Detfurth Sandstone and Lower Volpriehausen Sandstone members. All maps are provided in PDF format for presentation purposes (Annex B, C, K). Ascii-gridfiles (ZMAP- and ARCGIS-format) of the surfaces and ZMAP lines files of the faults can be downloaded from the nlog site. In addition to the depth and thickness maps, 3 structural cross sections from the major stratigraphic units (2 NE-SW and 1 W-E direction) are generated from the 3D model (Annex G). The cross sections are provided in PDF-format only.

3.4 Basin modelling

The basin modelingprogramme Petromod (version 10) of IES was used to visualise and analyse the 1D-3D geological, geothermal, compaction, pressure and fluid flow evolution of the area in relation to the evolution of the petroleum systems (maturity, generation, migration and accumulation of oil and gas). The data analysis presented in chapter 3 provided the input data, and the calibration data required for the numerical modelling.

Initially 1 D simulations at about 30 well locations were carried out to verify conceptual models of subsidence and erosion history.

The 3D basin modelingrequires the definition of the uninterrupted time-stratigraphic sequence of events during the evolution of the study area. The present-day 3D geological model was the basic input for the 3D modelling. Depth and thickness maps were loaded from Petrel into Petromod and horizons were adjusted. The present-day stratigraphic model was refined with additional maps of two reservoirs (Lower Detfurth Sandstone Member, Lower Volpriehausen Sandstone Member) and the source rock (Posidonia Shale Formation). Layers were split to include additional reservoir and sealing units (Solling Formation reservoir and sealing evaporites of the Röt Formation in the Upper Germanic Trias Group; Terschelling Sandstone Formation in the Schieland Group). Facies maps were created to take lateral facies changes into account (Upper Rotliegend Group, Solling Formation).

The stratigraphic model was extended with the StepGraben and Hospital Ground, Maurits, Ruurlo and Baarlo formations of the Limburg Group with estimated present-day thicknesses of 0 – 250 m for the Step Graben & Hospital Ground, 0 – 200 m for the Maurits, 0 – 400 m for the Ruurlo and 100 – 200 m for the Baarlo formations; erosion phases defined and erosion maps created; and lithotypes assigned to each layer.
The detailed information about the basin modelingprocess and the results will be in Verwey et al. 2009, which will be published later this year.

4 Present-day 'setting'

4.1 Geological framework

The dominant features of the present-day structural framework and lithostratigraphic build-up reflect its complex tectonic history of the area (Annexes E, F and G).
The main structural elements in the area are of Mesozoic origin: the Dutch Central Graben and the Terschelling Basin, as well as the adjacent Central Offshore Platform, Vlieland High and Ameland Block (Figure 4.1.1). The northwestern extension of the Lauwerszee Trough of Variscan origin reaches the southern border of the area.

The Cenozoic sedimentary fill of the Southern North Sea Basin covers the Mesozoic structural elements that rest on the Southern Permian Basin which in turn overlies the Variscan Basin. The associated tectono-stratigraphic sequences are separated by the three major phases of tectonic activity and erosion (Annex F), namely the Saalian, Mid-Kimmerian and Subhercynian tectonic phases.

4.1.1 Structural framework

The basin boundary fault zones of the Terschelling Basin and the southern part of the Dutch Central Graben in combination with the fault-associated salt structures form the structural framework of the area.

Faults
The major boundary fault zones that could be interpreted from seismic data include (Annex E, Figure 4.1.1)
Rifgronden Fault Zone. The WNW-ESE trending fault zone is the northern boundary of the Terschelling Basin. This fault zone shows dextral offsets (De Jager 2007);
Hantum Fault Zone. The WNW-ESE oriented northern part of this fault zone is the southern boundary of the Terschelling Basin. The Hantum Fault Zone extends southeastward and forms the western boundary of the Lauwerszee Trough. In the study area faults in the Hantum Fault Zone show vertical offsets at the base of the Zechstein Group of up to 1500 m. The fault zone is composed of two fault systems: 1) WNW-ESE synthetic strike slip faults, and 2) NW-SE antithetic strike slip faults (De Jager 2007).
NNE-SSW trending boundary fault zone between the Terschelling Basin and the Dutch Central Graben.
NNE-SSW trending boundary fault zone between the Dutch Central Graben and the Cleaver Bank High.
WNW-ESE trending fault zone along the southern boundary of the Dutch Central Graben.

The structural grid shows a dominance of two directions: NNE-SSW and WNW-ESE. Different phases of fault activation and reactivation were identified. The old Hantum Fault Zone has been active since the Late Carboniferous, and was reactivated multiple times during the Triassic and Late Jurassic. The Rifgronden Fault zone may be a similar repeatedly reactivated fault zone (De Jager 2007).

The NNE-SSW oriented faults were active during the early Kimmerian tectonic phase (Late Triassic) in an extensional stress regime. Both NNE-SSW and WNW-ESE trending faults were active during the Mid-Late Kimmerian phases (Late Jurassic) in a trans-tensional stress field and during the Subhercynian phase (Late Cretaceous) in a transpressional stress field (tectonic inversion). Cenozoic fault offsets recognised in the post-Zechstein sequence are mainly related to active salt deformation.

The Zechstein salt acts as a major detachment zone because of its great thickness and visco-plastic behaviour and often separates sub-salt fault systems from the faults in the overburden. Deep reaching basin boundary faults, such as the Hantum Fault Zone and possibly also the Rifgronden Fault Zone were already established in the Early Permian and reactivated later. New faults below base Zechstein were generated during the post-Zechstein tectonic phases. The creation and activity of faults in post-Zechstein sedimentary sequences result from basement faulting and are locally enhanced by salt doming. Minor reverse faults in the post-Zechstein sediments occur near the boundaries of the Terschelling Basin. These faults are most likely related to Late Cretaceous inversion.

Salt structures

Salt deposits occur in the Late Permian Zechstein Group and in the Triassic Röt, Muschelkalk and Keuper formations. The presence of Zechstein salts greatly influenced the post-Permian structural and sedimentary development of the area. The original estimated depositional thickness of the Zechstein Group was 650 m (ZE1 to ZE4 formations), a thickness extrapolated from wells in undisturbed areas, like Uithuizermeeden-01 (Van Adrichem Boogaert & Kouwe, 1992-1997). Its present-day thickness varies from approximately 5000 m in salt domes and structures to only a few metres in withdrawal areas. The larger part of the area is regarded as a salt depletion area, where salt has moved away laterally and vertically into salt structures and is still moving.

About 30 – mainly Zechstein – salt structures were identified, including salt pillows, salt walls, diapirs and salt tongues, with greatly varying dimensions (length between 5-30 km, width up to 8 km, height up to 5 km).

Salt structures follow the structural grain of the area. For example, NNE-SSW-trending salt walls closely follow basin boundary faults of the Dutch Central Graben and the Terschelling Basin (see also Remmelts 1996). In the platform areas halokinesis resulted in salt pillows only.

Timing of salt movement could be related to phases of active fault movement (see also Remmelts 2006). Halokinesis started already in the Early and Middle Triassic. The salt movement during the Late Triassic occurred along the boundary between the Terschelling Basin and the Dutch Central Graben and at the eastern border of the Terschelling Basin (block M05). A subsequent major phase of salt movement in the Dutch Central Graben took place during the Callovian, Oxfordian and Kimmeridgian, while it occurred later in the Terschelling Basin, namely during the Portlandian and the Ryazanian (salt structures in blocks M02, -05, L04,-05). This Late Jurassic phase of halokinesis resulted in piercing of many of the salt structures.

A Late Cretaceous-Early Tertiary phase of reactivation of the salt structures along the boundary between the Terschelling Basin and the Dutch Central Graben and in the Terschelling Basin (blocks M02, -05, L04,-05) could be identified. The salt structures in the Terschelling Basin remained active during the Late Tertiary until present.

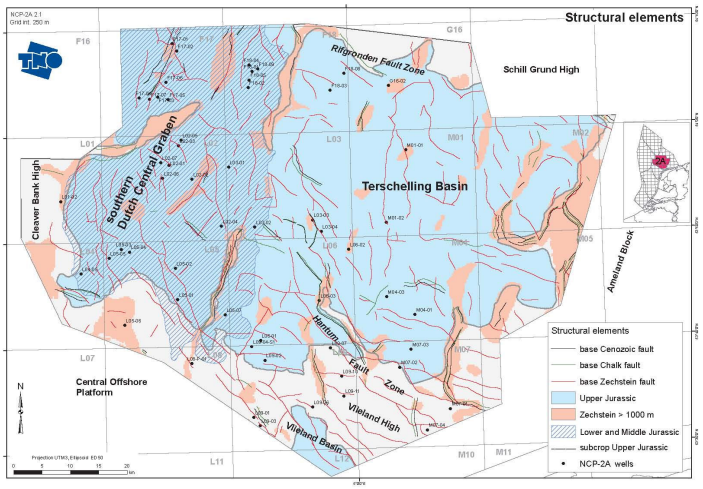

Figure 4.1.1 Main structural elements (see also Annex D)

4.1.2 Stratigraphy

The well logs of all 80 selected wells were loaded into Petrel and lithostratigraphically (re-) interpreted on member level. For this purpose several correlation panels (Annex I) have been constructed, some on group level to facilitate detailed interpretation. Others were set up with a spatial distribution to create a more regional view. A tectono-stratigraphic chart for this specific area was constructed (Annex F, Figure 4.1.2). Furthermore, other sources like biostratigraphy, core descriptions, consultancy reports and specific literature have been used to enhance and improve the litho- stratigraphic interpretation. The main characteristics of the stratigraphic buildup is described per stratigraphic group. Annex B and C present the depth and thickness maps of the groups.

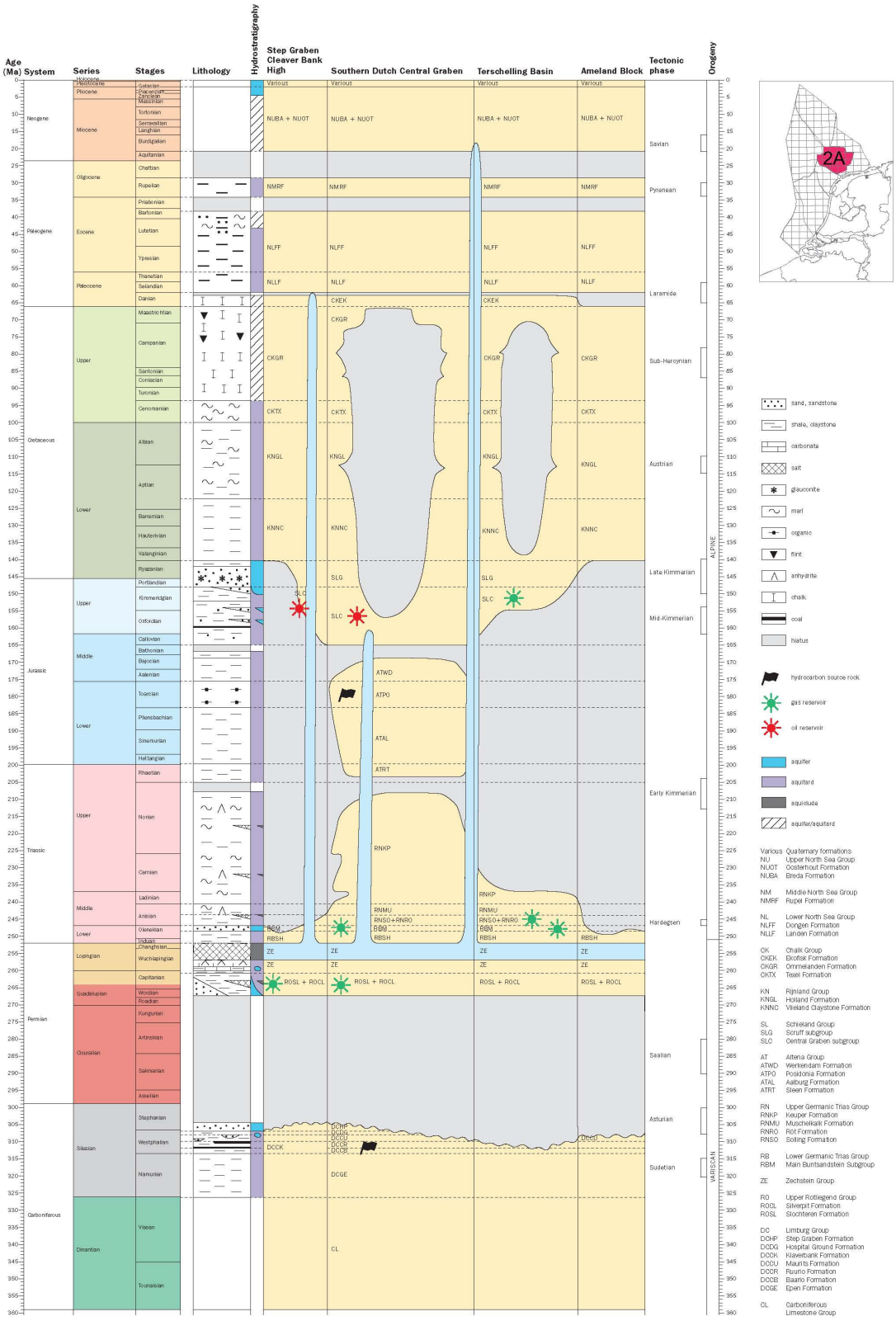

Tectono-stratigraphic chart of the Dutch Central Graben and Terschelling Basin. Time scale according to Gradstein et al. (2004).
The subdivision of the Upper Jurassic presented here does not follow the official stratigraphic nomenclature of the Netherlands (Adrichem Boogaert & Kouwe, 1997). In this study the Schieland Group (SL) is subdivided into the Scruff subgroup (SLG) and the Central Graben subgroup (SLC).
The Scruff subgroup relates to the former Scruff Group while the Central Graben subgroup relates to the former Schieland Group.

Figure 4.1.2 Tectono-stratigraphic chart of the Dutch Central Graben and Terschelling Basin (see also Annex F)

Limburg Group

Only a few wells in the area reached the Limburg Group due to its deep burial. The burial depth of the top of the Limburg Group increases from SE towards NW and reaches depths of approximately 6000 m in the Dutch Central Graben. The base of the Limburg Group is at depths of 8-9 km. Most information on the lithostratigraphy of this group was deduced from regional mapping studies.

The sediments of the Limburg Group were deposited during the Silesian in an E-W oriented flexural foreland basin. This basin formed under the influence of the northward migrating Variscan thrust front and is bounded by the London Brabant Massif to the south and the Mid North Sea – Ringkøbing-Fyn High to the north (Van Buggenum and Den Hartog Jager 2007; Ziegler 1990).

At the largest scale, the Limburg Group shows an overall regressive cycle associated with the filling of the Variscan foredeep basin. The lower part is defined by the largely marine claystones of the Geul subgroup (Namurian to Earliest Westphalian A). On top the Geul subgroup are the Caumer, Dinkel and Hunze subgroups which show a transition towards more continental and finally arid conditions. The Caumer subgroup (Namurian B – Westphalian C) marks the onset of peat (coal) deposition in a deltaplain / swamp environment. In this subgroup the Klaverbank Formation represents the proximal, coarser-grained fluvial and deltaic sandstones, whereas the Baarlo and Ruurlo formations comprise the more distal fine-grained sediments, including coal layers.

The Maurits Formation of the Caumer subgroup represents the lacustrine and floodplain fines with prolific coal formation. The transition to more fluvial conditions during the Westphalian C/D resulted in the deposition of the sandstone dominated Dinkel subgroup (Hospital Ground Formation). Finally the conditions become arid as shown by the occurrence of red beds in the Hunze subgroup (Step Graben Formation).

The Asturian tectonic phase (Westphalian C/D to Stephanian) resulted in differential movements and subsidence of the Proto Central Graben area.
The Carboniferous deposits underwent strong uplift and subsequent erosion during the Saalian thermal uplift (Early to Middle Permian) the effect of which is displayed in the Pre-Permian subcrop map (Figure 4.1.3). In most of the area the Permian is underlain by the Ruurlo Formation. To the southwest the deposits become younger with the occurrence of the Maurits, Hospital Ground and Step Graben formations. The oldest deposits (Baarlo Formation) subcrop in the south-east corner of the area (Block M07).

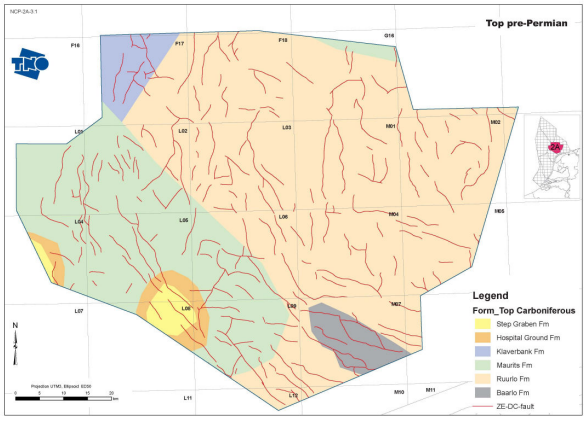

Figure 4.1.3 Top Carboniferous (based on Mijnlieff 2002)

Upper Rotliegend Group

The few wells that penetrate the Upper Rotliegend Group are located along the southern edge of area where sandstone layers occur more frequently. The Saalian Unconformity separates the sediments of the Upper Rotliegend Group from the Limburg Group. The hiatus spans some 50 Ma in the study area.

Following the Saalian phase of uplift and erosion, clastic deposition in the Netherlands started in the latest Middle Permian and lasted until the earliest Late Permian. Sediments were deposited under arid conditions in a large E-W trending complex of continental sedimentary basins known as the Southern Permian Basin, which stretched from the British Isles into Poland. The Dutch on- and offshore areas primarily received their sediments from the Variscan mountain belt to the south.

The Upper Rotliegend Group is subdivided into the Slochteren Formation comprising mainly fluvial and eolian sandstones and conglomerates, and further to the north the Silverpit Formation which is composed of claystones, siltstones and evaporites deposited in a playa / lake environment. The formations are lateral equivalents.

The study area is located just north of the narrow transition zone between both formations and mainly comprises the fine grained sediments of the Silverpit Formation. Along the southern margin of the area minor occurrences of the Upper and Lower Slochteren members were encountered.

Figure 4.1.4 shows that the thickness of the Upper Rotliegend Group increases northwards.
The Upper Rotliegend is conformably overlain by Late Permian marine carbonates and evaporites of the Zechstein Group.

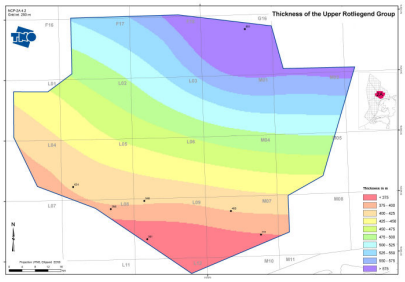

Figure 4.1.4 Thickness of the Upper Rotliegend Group

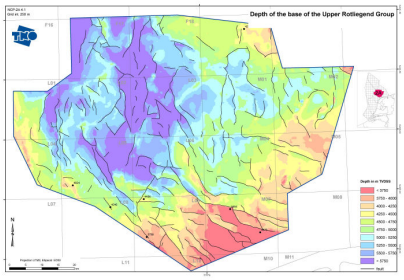

Figure 4.1.5 Depth base of the Upper Rotliegend Group

Zechstein Group

The Zechstein Group deposits result from a series of marine transgressions into the Southern Permian Basin, each transgression followed by an evaporation phase. The Zechstein Group consists of four to five evaporite cycles. The Zechstein Upper Claystone Formation covers these cycles unconformably. In the mapped area, only the succession of the Z1 Formation is undisturbed, whereas most of the Z2, Z3 and Z4 cycles have been deformed by halokinese.

The Z1 cycle is composed of the Kupferschiefer, a thin organic-rich shale at the base, followed by the Z1 Carbonates Member. The Z1 Werra Anhydrite was deposited on the anhydrite platform (Geluk, 2007a) that extended from the northern onshore area into the offshore, including the entire mapped area. The Z2, Z3 and Z4 cycles were originally deposited with claystone and/or carbonate at the base, followed by the deposition of anhydrite and salt and sometimes overlain by a roof anhydrite. Their internal succession is deformed by salt flow. The various members are concentrated in deformed state in the salt domes and salt walls. In between the salt structures most of the sequences are squeezed out. The Zechstein Upper Claystone Member is generally present between salt structures and absent above the structures.

In the Terschelling Basin and southern Dutch Central Graben salt deformation occurred multiple times. The original estimated depositional thickness of the Zechstein Group was 650 m, while its present-day thickness varies from approximately 5000 m in domes to only a few metres in withdrawal areas (Figure 4.1.5). The larger part of the area is regarded as a salt depletion area, where salt has moved away laterally and vertically into salt structures.

The burial depth of the base of the Zechstein Group increases from 3000 – 4500 m in the eastern part of the area to more than 5000 m in the Dutch Central Graben (Figure 4.1.6).

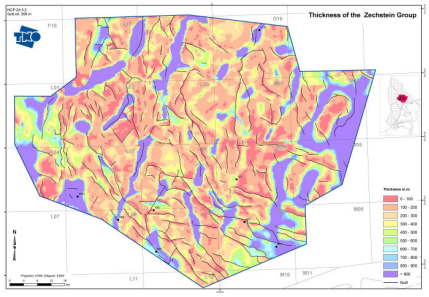

Figure 4.1.6 Thickness of the Zechstein Group

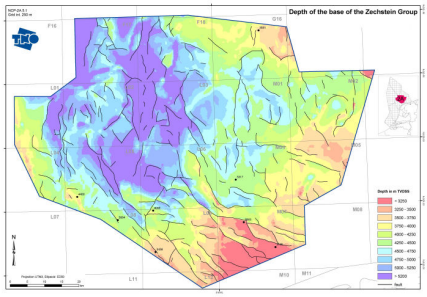

Figure 4.1.7 Depth base Zechstein Group

Lower and Upper Germanic Trias groups

After the deposition of the Zechstein Group the sedimentation of the Early Triassic rocks took place in a similar basinal setting but under continental conditions. The depositional environment in the mapped area is interpretated as lake to lake-margin (Geluk, 2007b). Restricted marine conditions returned during Middle and Late Triassic times.

Two major groups of sediments are recognised in the Triassic rocks: the Lower and Upper Germanic Trias groups. The boundary between these two groups is formed by the Hardegsen or base Solling Unconformity.
The Lower Germanic Trias Group (Indian to Olenekian age) is mainly a clastic succession. It consists of fine-grained siliclastic deposits with oolite intercalations in the lower part of the succession and more sandbodies alternating with claystones and siltstones in the higher parts of the succession. It is subdivided from bottom to top in the Main Claystone and the Rogenstein formations and the Main Buntsandstein subgroup containing the Volpriehausen, Detfurth and Hardegsen formations.
The Lower Germanic Trias Group is present in most of the area, with the most complete succession in the proto-Dutch Central Graben. It is affected by later halokinesis of the Zechstein salt. Only six wells have penetrated the base of the Lower Germanic Trias Group.

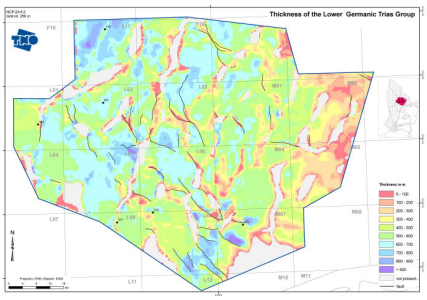

Figure 4.1.8 Thickness of the Lower Germanic Trias Group

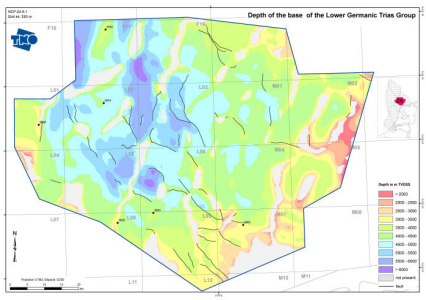

Figure 4.1.9 Depth base Lower Germanic Trias Group

The Lower Volpriehausen and Detfurth Sandstone members have their greatest thickness in the graben (Figures 4.1.10 and 4.1.11).

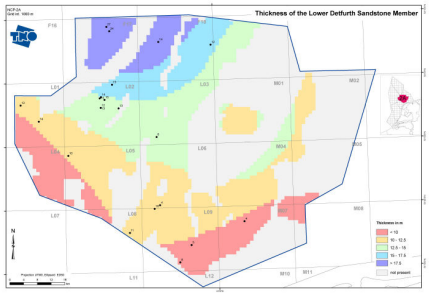

Figure 4.1.10 Thickness of the Lower Volpriehausen Sandstone Member

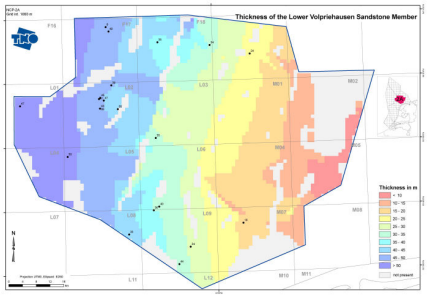

Figure 4.1.11 Thickness of the Detfurth Sandstone Member

The Upper Germanic Trias Group (Anisian – Norian age) consists of 4 formations: the Solling, Röt, Muschelkalk and Keuper formations. The sediments were deposited under continental to restricted marine conditions. All formations are present in the mapped area.
The Solling Formation has an anomalous sequence built-up in quadrants L09 and L06. Hugh sand deposits (mainly eolian sandstones) up to 165 m thickness, the so-called Solling Fat Sandstone, have been deposited in very restricted areas (Figure 4.1.12). The accommodation space was created by syn-sedimentary fault movements in combination with fault related halokinese. The process of sand deposition is described by Jager and Geluk (2007b).

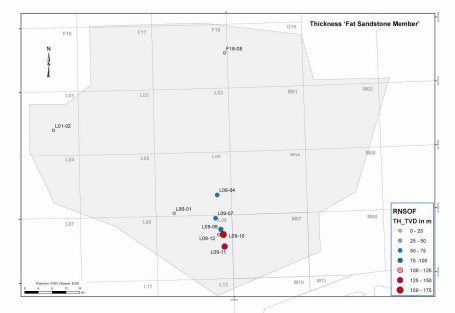

Figure 4.1.12 Thickness of the Solling Fat Sandstone

The Röt Salt is widely present, but there is a lateral transition into anhydrite towards the southern edge of the area (Figure 4.1.13).

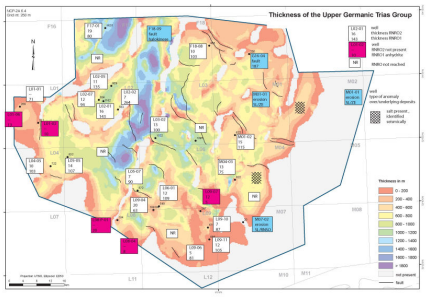

Figure 4.1.13 Thickness of the Upper Germanic Trias Group, including information on distribution and thickness of the salt members of the Röt Formation.

The present-day distribution of the sediments of Muschelkalk and Keuper formations is restricted to the later Jurassic-Cretaceous rift basins. The complete Muschelkalk succession is present in the Dutch Central Graben and partly eroded in the Terschelling Basin. The Keuper Formation is only present in the graben.

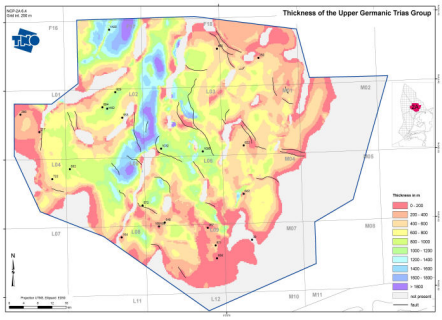

Figure 4.1.14 Thickness of the Upper Germanic Trias Group

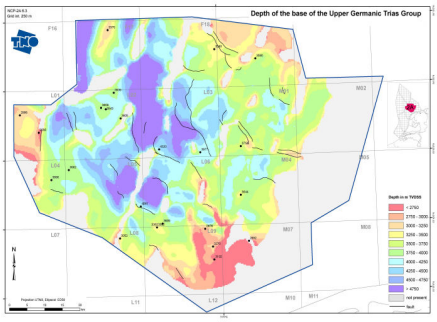

Figure 4.1.15 Depth base Upper Germanic Trias Group

Altena and Schieland and Scruff groups

The present-day distribution of the Altena Group is confined to the Dutch Central Graben. These Lower to Middle Jurassic sediments range from Rheatian to Oxfordian and are predominantly marine. In origin the Upper Jurassic Schieland and Scruff groups are present in the Dutch Central Graben and the Terschelling Basin. Their depositional environment varies from continental to restricted marine.

After the Early Kimmerian phase the basinal structure of the area changed into fault bounded basins and highs. Early in the Middle Jurassic the thermal Central North Sea Dome developed, resulting in the Mid-Kimmerian uplift. In the mapped area these movements caused deep erosion with only Lower to early Middle Jurassic deposits preserved in the Dutch Central Graben.

The succession of the Lower to Middle Jurassic sediments, encountered in the wells in this area, consists of the Aalburg Formation, Posidonia Shale and Werkendam formations. The Brabant Formation has not been penetrated in this area. In between salt domes the thickness of the Altena Group is more than 1000 m. There is no well control in this specific area, but on the seismic profiles there is no indication that the Brabant Formation with its characteristic limestone beds is present in this area. We assume that the massive thickness is caused by rapid creation of accommodation space due to halokinesis in combination with marine transgression.

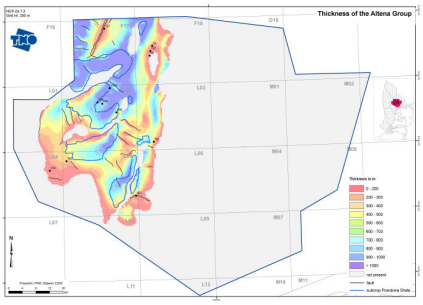

Figure 4.1.16 Thickness of the Altena Group

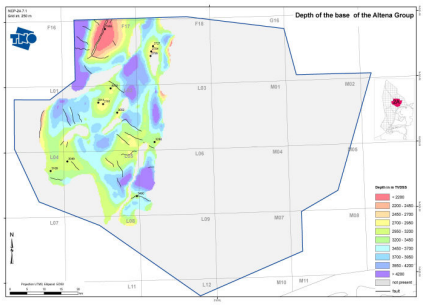

Figure 4.1.17 Depth base Altena Group

The Posidonia Shale Formation, with its organic-rich layers is only encountered in some isolated spots in the Dutch Central Graben. It serves though, as the source rock for five oil fields in this area.

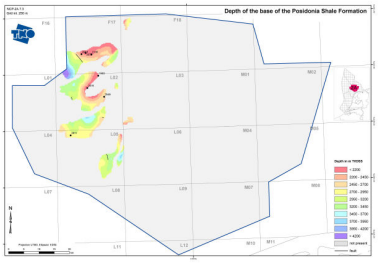

Figure 4.1.18 Depth base Posidonia Shale Formation

The Upper Jurassic sediments were deposited in syn-rift structures, which led to enormous variations in thickness and fast changing depositional settings (TNO-report 2006-U-R0191/A and Wong 2007).
The Schieland and Scruff groups have been interpreted based on well log data, biostratigraphical data, sedimentological data and on seismic marker ‘B3’ which corresponds with the base of tectono-stratigraphic unit 3, base Scruff Group (Annex H). In this study a tectono-stratigraphic framework was constructed for the study area and an attempt was made to create a new subdivision for the Upper Jurassic sediments in conjunction with and elaborating on Abbink et al. (2006).

Initially a distinction was made between the terrestrial and marine deposits, resulting in a Schieland Group comprising a Central Graben subgroup (terrestrial) and a Scruff subgroup for all marine sediments (viz. Annex H). Many problems were encountered and it was decided to introduce a new subdivision until all Upper Jurassic-Lower Cretaceous basins were mapped. After finishing this offshore mapping program in 2010 a separate, profound study will be executed. As a result some of the naming of the groups, subgroups and formations in this report are not entirely conform the nomenclature by Van Adrichem Boogaert and Kouwe (1992-1997).

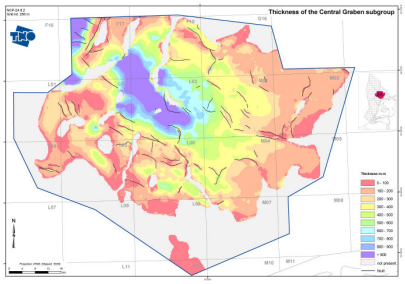

4.1.19 Thickness of the Central Graben Subgroup of the Schieland Group

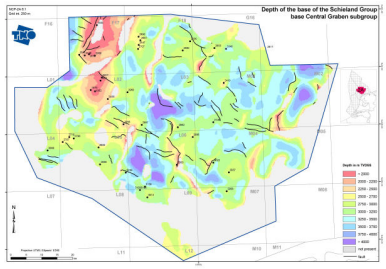

4.1.20 Base Schieland Group, Central Graben Subgroup

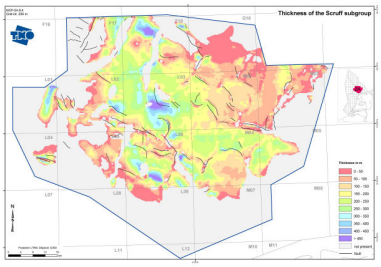

4.1.21 Thickness of the Scruff Group

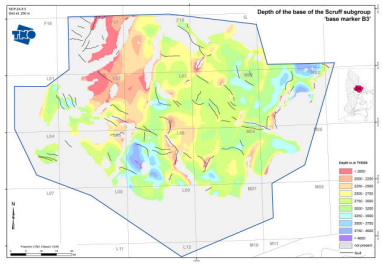

4.1.22 Base Scruff Group

The deposits consist of fine-grained material with coal seams, sand and claystones. In the southern Central Graben and the Terschelling Basin rapid lateral changes of lithology and facies were encountered. For this reason a sedimentological study was carried out to get a better grip on the relation between the deposits and the depositional environment of tectono-sequence 2, Annex H and TNO-report 2006-U-R0191/A).

This study revealed five depositional environments: 1) lower delta plain 2) restricted lagoon 3) open lagoon 4) barrier system and 5) shallow marine. These depositional environments change in time as is illustrated in 4.1.23.
After construction of thickness maps, three time-slices were created, that show a change from delta plain deposits in time-slice 1, developing into a complex of delta plain deposits grading into lagoonal, barrier and shallow marine deposits in time-slice 2, and the final stage with marginal-to-shallow marine deposits.

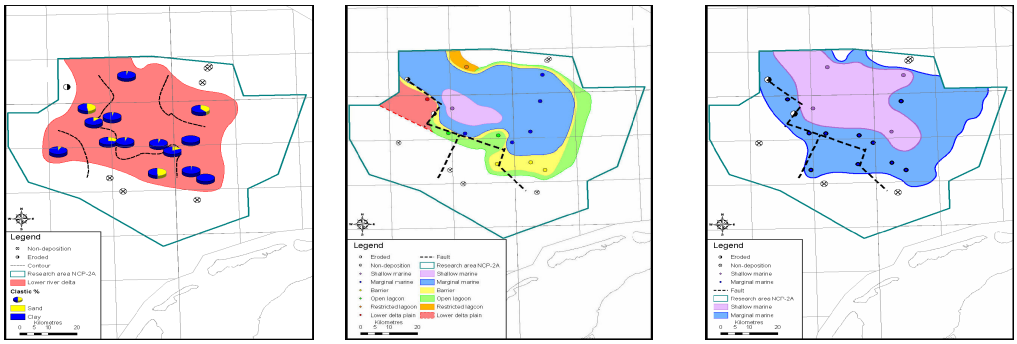

initial stage ***middle stage*** ***final stage***

Figure 4.1.23 Development in time of depositional environments in tectono-sequence 2 of the 'Upper Jurassic' sediments.

In the Dutch Central Graben subgroup and Friese Front Formation of the Schieland Group five oil fields developed. In the Terschelling Basin two fields are gasbearing viz. L06 with the Terschelling Sandstone Member as reservoir and G16 with the Scruff Greensand Formation as reservoir.

Rijnland and Chalk groups

The Rijnland Group is deposited in the entire 2A area. The greatest depths and thicknesses can be found along the flanks of salt domes and walls, indicating that the salt movements partly controlled the sedimentation.
The Chalk Group in its present-day setting is absent in the Dutch Central Graben or thin in the central part of the Terschelling Basin, showing the Subhercynian inversion axis which is NS in the graben with an NW-SE extension to the Terschelling Basin. The greatest depth and thicknesses are located on the former platforms, such as Ameland Block, Schill Grund High and Central Offshore Platform.

After the Kimmerian rifting phases a period with regional subsidence commenced. In the Early Cretaceous sedimentation took place not only in the former basins but also on platforms and highs due to global sea-level rise. In area 2A this overall transgression resulted for a large succession of mainly clay- and siltstones. During Aptian times deeper marine conditions dominated and calcareous claystones were deposited. In the Late Cretaceous the hinterland had been flooded almost completely and hardly any clastic influx occurred in the basin.

The Vlieland Claystone Formation of the Rijnland Group comprises fine-grained material like clay- and siltstones. In the 2A area the top of the Vlieland Claystone is calcareous and where very pronounced, this interval can be placed in the Vlieland Marl Member.
Most of the formerly interpreted Friesland Sandstone Member of the Rijnland Group has been re-interpreted as Scruff Greensand Formation of Late Jurassic age. The Holland Formation is represented by the Lower and Upper Holland Marl members separated by the Middle Holland Claystone Member.

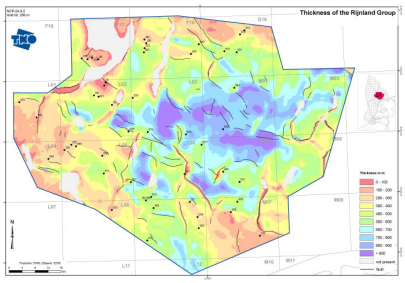

Figure 4.1.24 Thickness of the Rijnland Group

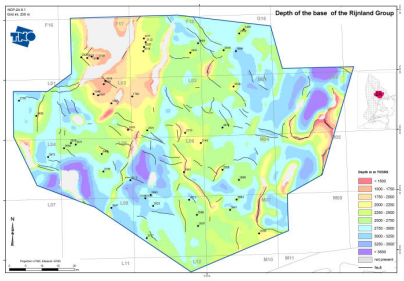

Figure 4.1.25 Depth base Rijnland Group

The Chalk Group is present with the Texel, Ommelanden, and Ekofisk formations. In the inverted area the Ekofisk Formation lies unconformably on the Rijnland Group. The deposits consist of a thick succession of carbonate rocks. The bulk of the group comprises bioclastic limestones and marly limestones. Originally, these limestones had a more chalky nature, but as a result of deep burial they were compacted strongly and became denser. Locally, in the F17 quadrant glauconitic sands occur in the Santonian. Chert concretions are particularly present at the top of the Ommelanden as well as the |Ekofisk formations. On the flanks of the inversion axis the Chalk sequence is often present in a condensed form like in well L03-02. In the northeast and southwest, the former platform areas, the Chalk Group can reach thicknesses of more than 1200 m.

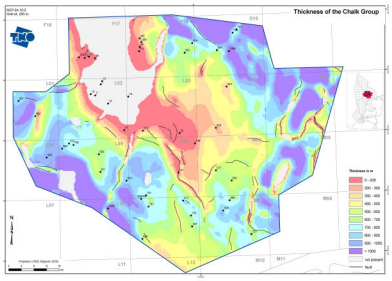

Figure 4.1.26 Thickness of the Chalk Group

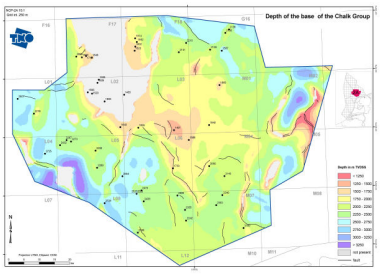

Figure 4.1.27 Depth base Chalk Group

The Lower and Upper Cretaceous deposits in the mapped area don’t show any hydrocarbon accumulations.

Lower, Middle and Upper North Sea groups

The Lower, Middle and Upper North Sea groups are present in the entire area. The deposits of the Lower and Middle North Sea Group have their greatest thickness in the southwest; the deposits of the Upper North Sea Group the northwest. Salt movement greatly influenced the depositional thickness of the Lower and Middle North Sea groups, while the base of the Upper North Sea Group is only affected by break-through of the domes. In the formerly inverted area in the NW of the area the Lower and Middle North Sea groups are relatively thin, while the deposits of the Upper North Sea Group show a considerable increase in thickness.

After the Mesozoic rifting phases and the Subhercynian and Laramide inversion phases the siliclastic sediments of the Lower, Middle and Upper North Sea groups were deposited in the large, rapidly subsiding epicontinental basin, the North Sea Basin, which formed in response to thermal relaxation, isostatic adjustment and sea level rise. In the mapped area the sediments were deposited in a marine environment.

The deposition of the North Sea Supergroup has been effected by salt movements. The sediments show greater thicknesses in rim-synclines. In Late Miocene and Pliocene times the former Dutch Central Graben shows an accelerated subsidence, resulting in an enormous accomodation space for the deposits of the Eridanos river system that reached the mapped area in the Pliocene. Over 1000 m of sediments were deposited in the northwestern part of the mapped area. (Overeem et al., 2001)

The North Sea Super Group consists of three groups, viz. the Lower, Middle and Upper North Sea Group. The Lower North Sea Group is divided into the Landen and Dongen formations. At the base of the Dongen Formation a mixture of clay, silt and volcanic ash form the Basal Dongen tuffite. The Lower North Sea Group consists mostly of clay(-stone) with marly deposits in the Brussels Marl Member. The Middle North Sea Group consists of clay(-stone) of the Rupel Formation. Sandy deposits prevail in the Upper North Sea Group. Especially the Pliocene sands consist of pro-delta stacked sands; the overall trend is coarsening-up. The overlying Quaternary deposits are incorporated in the Upper North Sea Group.

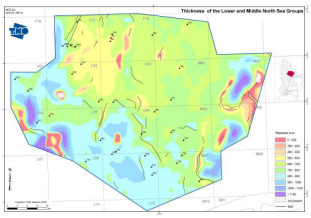

Figure 4.1.28 Thickness of the Lower and Middle North Sea groups

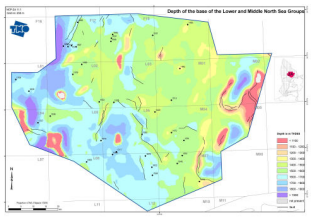

Figure 4.1.29 Depth base Lower North Sea Group

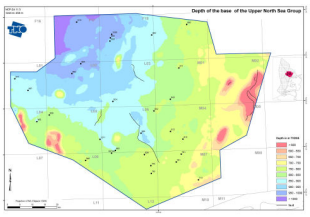

Figure 4.1.30 Depth base Upper North Sea Group

4.2 Hydrogeological setting

4.2.1 Hydrogeological framework

The hydrogeological framework describes the spatial distribution of the permeability of the subsurface. The framework is characterised by the distribution, thickness and dip of hydrostratigraphic units (aquifers/reservoirs, aquitards and aquicludes) and the location of the geological structures and tectonic elements of importance for subsurface fluid flow. Annex F shows the generalised present-day hydrostratigraphy of the Terschelling Basin and the southern part of the Central Graben.

The more permeable hydrostratigraphic units consist of sands, sandstones and limestones. Aquifers largely coincide with the reservoir units and include:

- The sandy Hospital Ground and Step Graben Formations of the Limburg Group; erosional remnants of these formations were encountered in the southwesternmost part of the area;
- The sandy Lower Slochteren Member of the Upper Rotliegend Group; the northernmost extension of this member reaches the southwesternmost part of the area;
- Carbonate Members of the Zechstein Group;
- The Lower Detfurth and Lower Volpriehausen Sandstone Members of the Lower Germanic Trias Group; large distribution;
- The Solling Fat Sandstone Member of the Upper Germanic Trias Group; its distribution is mainly confined to blocks L06 and L09, scattered presence in blocks L01 and F18;
- Several sandy lithostratigraphic units in the Jurassic Schieland Group (Terschelling Sandstone Member, Scruff Greensand Formation, Friese Front Formation); the Terschelling sandstones are regionally present;
- Quaternary sands of the Upper North Sea Group. The permeability of the Chalk Group varies and both aquifers and aquitards occur in the Chalk (e.g. Verweij 2006).

The most important low permeable units controlling pressure and flow conditions are the salt members of the Zechstein Group, the evaporite members of the Upper Germanic Trias Group (such as the Main Röt and Upper Röt Evaporite Members of the Röt Formation), and in the northern parts of the area also the Silverpit Evaporite Member of the Upper Rotliegend Group. Shaly deposits of low matrix permeability occur throughout the entire stratigraphic sequence (Annex F).

The claystones and the salt members separate the main aquifer/reservoir units. The numerous large Zechstein salt structures, and also the major faults, disrupt the lateral continuity of the pre-Tertiary sedimentary sequences. Based on the 3D permeability distribution, the area can be subdivided into 4 hydrostratigraphic domains:

- Deep basin hydrostratigraphic domain 1 capped by the salts of the Zechstein Group (and in part by the Silverpit Evaporites) (this domain includes the Upper Rotliegend Group and the Limburg Group);
- Hydrostratigraphic domain 2, consisting of hydrostratigraphic units that overly the Zechstein salt and are laterally not hydraulically restricted by Zechstein salt structures;
- Hydrostratigraphic domain 3, consisting of hydrostratigraphic units that overly the Zechstein salt and are laterally hydraulically restricted by – especially – Zechstein salt structures;
- Hydrostratigraphic domain 4, consisting of Triassic units that overly the Zechstein salt and are laterally hydraulically restricted by – especially – Zechstein salt structures, and capped by evaporites of the Upper Germanic Trias Group.

Domain 1 is present in the entire area; domain 2 in the platforms and highs along the southern edges of the study area (Cleaver Bank High, Central Offshore Platform, Vlieland High); and domains 3 and 4 in southern Central Graben and in the Terschelling Basin.

4.2.2 Salinity

The composition of water samples from 6 wells in the studied area indicate that the formation waters of Upper Permian to Cretaceous reservoir units are chloride-dominated brines with salinities well in excess of sea water salinity.

Figure 4.2.1 is a cross plot of the change of formation water salinity versus depth (salinity as used here is synonymous with total dissolved solids, i.e. TDS). The plotted salinity information is derived from water sample analyses and from pressure data using the pressure gradient calculation method (Underschultz et al. 2002). The cross plot shows that formation water salinities in the Upper Rotliegend to Cretaceous reservoir units at depths of more than 1500 m range from approximately 90 000 mg/l to more than 300 000 mg/l. Large variations in salinity occur in the Jurassic and Triassic units at the same depth of measurement. In the study area abundant amounts of salts (evaporites of the Silverpit Formation, Zechstein Group and Upper Germanic Trias Group) are available for dissolution and for increasing the salinity of formation water. The large salt structures bounding the Terschelling Basin and the southern Dutch Central Graben are laterally in contact with aquifer/reservoir units of Triassic to Cretaceous age and may explain the observed large variations of salinity at the same depth of measurement.

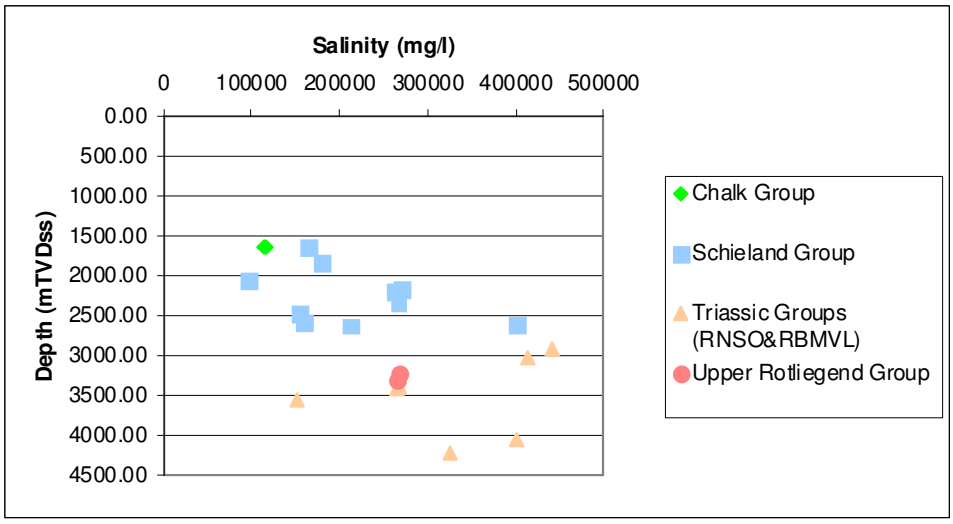

Figure 4.2.1 Cross plot of formation water salinity per stratigraphic unit.

The density of the formation water also varies significantly as a consequence of these large variations in salinity. This is of importance, amongst other things, because water density affects the formation water pressures.

4.2.3 Pressures

Introduction

The present-day pressures reflect both a) present-day active and/or paleo pressure influencing mechanisms, such as sedimentation, erosion, fluid flow, and b) the hydraulic characteristics (pemeability and compressibility) of the subsurface. Here we concentrate on the description of the distribution of observed pressures in relation to the present-day permeability framework.

The pressure-depth plots (Figures 4.2.2 and 4.2.3), Table 4.2.1, and the cross-sections (Figures 4.2.4,4.2.5 and 4.2.6) show the variation in pore fluid pressure and excess fluid pressure from RFT tests in the Terschelling Basin and the southern part of the Dutch Central Graben.

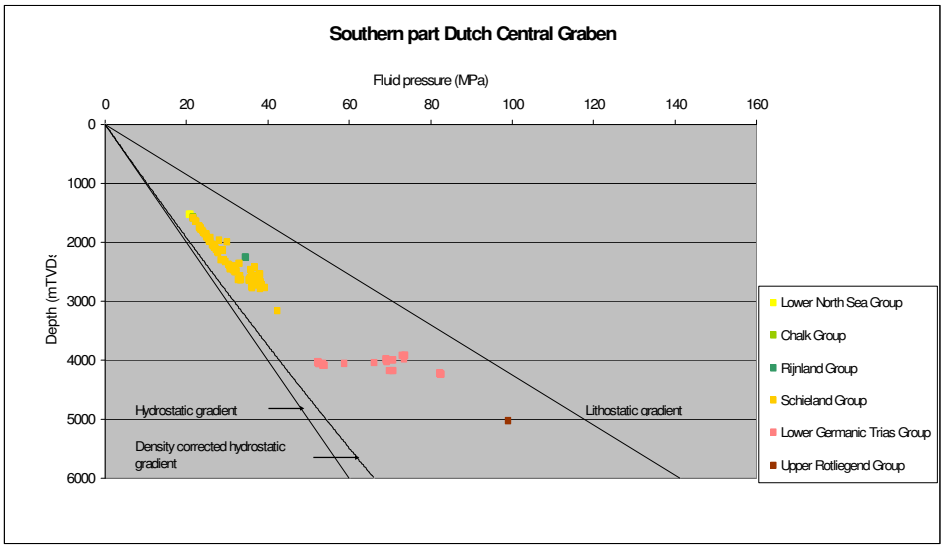

Figure 4.2.2 Multi-well plot of fluid pressure versus depth in different lithostratigraphic units in the southern part of the Dutch Central Graben. The plot shows that the fluids are overpressured in each unit. Very large lateral variation in pressures occurs in the Triassic units.

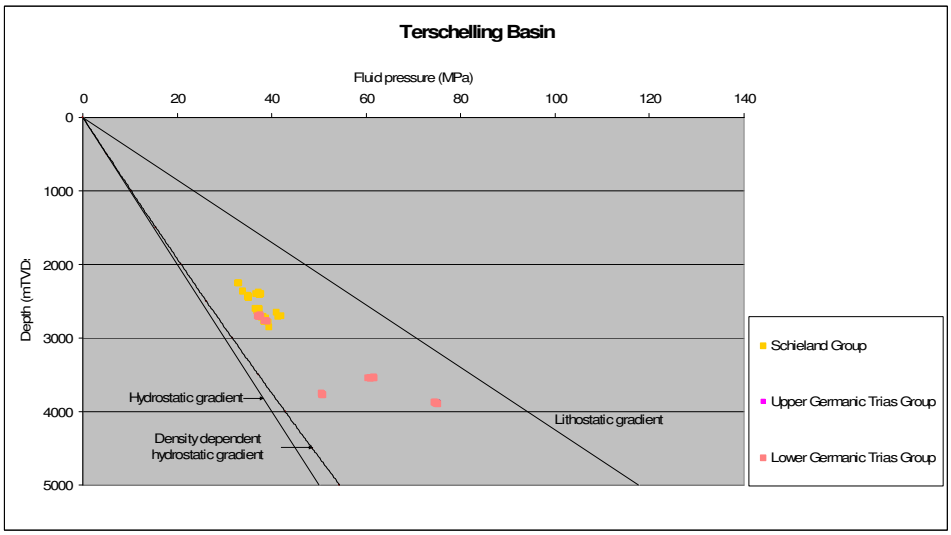

Figure 4.2.3 Multiwell pressure plot of fluid pressures in the Terschelling Basin. The plot shows that fluids are significantly overpressured in both the Schieland Group and the Triassic Groups.

The excess pressure – or overpressure – of pore water at a certain depth is the difference between the pore pressure and the hydrostatic pressure at that depth. The pressure-depth plots (Figures 4.2.2 and 4.2.3) show the vertical pressure distribution with depth for multiple wells per stratigraphic unit. These plots also show hydrostatic gradients. The hydrostatic gradient reflects the increase of hydrostatic pressure with depth.

The hydrostatic pressure of a pore fluid is given by $\rho_w gz$ (where z = depth, ρ_w = density of pore water, g = acceleration of gravity). The salinity of the pore water influences its density. The 'normal' hydrostatic gradient shown in the pressure-depth plots was calculated for sea water density, while the density-corrected hydrostatic gradient was derived from measured formation water salinities. It is common practice to report fluid overpressure values relative to a 'normal' hydrostatic gradient. The cross-sections (Figures 4.2.4, 4.2.5 and 4.2.6) show fluid overpressure values calculated in this way. It is important to realise that these values may reflect geological causes of overpressuring, the density contrast between a petroleum fluid and pore water (if the pressure was measured in a petroleum fluid), as well as pore water salinity effects. In order to exclude the effect of pore water salinity, we also calculated fluid overpressure values with respect to the density-corrected hydrostatic gradient. These values are shown in Table 4.2.1.

Table 4.2.1 Variation in fluid pressure and excess fluid pressure from RFT tests in the southern part of the Dutch Central Graben and the Terschelling Basin

Groups	Fluid pressure (MPa)	Excess fluid pressure*(MPa)	Depth (mTVDss)	Number of wells
SOUTHERN DUTCH CENTRAL GRABEN				
Lower North Sea	20.7-21.2	4.7-5.4	1526-1528	1
Chalk	21.6	5.3	1583	1
Rijnland	34.6	11.2	2253	1
Schieland	21.7-42.3	5-11.5	1595-3161	20
Lower Germanic Trias	52.3-82.7	9.1-37.1	3917-4248	8
Upper Rotliegend	99.0	44.2	5032	1
TERSCHELLING BASIN				
Schieland	32.9-42.0	9.2-13.7	2251-2859	6
Lower Germanic Trias	37.0-75.2	8.6-33.6	2704-3904	4

* Excess fluid pressure calculated in relation to the density-corrected hydrostatic pressure

Excess pressures

Table 4.2.1 and Figures 4.2.2 and 4.2.3 show that the pore fluids in the sediments of the Lower North Sea Group and older stratigraphic units in the studied basins are overpressured. The highest values of overpressure were observed in the Lower Germanic Trias Group in the Terschelling Basin (reaching 37 MPa) and the Upper Rotliegend Group in the southern Central Graben (exceeding 40 MPa). Large lateral variations in pressure occur in the Schieland Group and in the Lower Germanic Trias Group.

Depth exerts a first order control on the fluid pressures. The fluid pressures increase broadly parallel to the density corrected hydrostatic gradient at depths between 1500 and 2200 m in the southern part of the Central Graben (Figure 4.2.2), and fluid overpressures at these depths vary between 4.7 and 5.4 MPa (Table 4.2.1). At greater depths the lower-bound of the fluid pressures is no longer parallel to the density-corrected hydrostatic gradient. The fluid overpressure corresponding to the lower bound values reaches magnitudes of approximately 9 MPa at 4000 m.

There are no pressure measurements available at shallow depths (<2200 m) in the Terschelling Basin (Figure 4.2.3). The available pressure data show that the fluid overpressures at depths of 2250 m and beyond, all exceed 8 MPa (Table 4.2.1, Figure 4.2.3).

In addition to the above reported gradual increase of fluid overpressures at greater depths than 2200 m, there are significant lateral variations in overpressures in the Schieland Group in the Dutch Central Graben and in the Lower Germanic Trias Group in both basins (Table 4.2.1, Figures 4.2.2 and 4.2.3).

Excess pressures in the Schieland Group (hydrostratigraphic domain 3)

There is a clear spatial relation between the differences in fluid overpressure in the Schieland Group in the Dutch Central Graben and differences in thickness, and composition, of the low permeable units overlying the Schieland Group reservoirs (Figure 4.2.4). The fluid overpressures exceed 10 MPa in the Schieland Group reservoirs in the L01 and L05 blocks. These overpressures are maintained in the Schieland Group reservoirs by the low permeable claystones of the Schieland and Rijnland Groups, the Chalk Group and the claystones of the Lower North Sea Group.

In contrast, overpressures in the Schieland Group do not exceed 8.4 MPa in block F18 located in the inverted part of the Central Graben. The low permeable hydrostratigraphic units capping the reservoir in the inverted part of the graben is reduced in thickness due to erosion of the Chalk and the Rijnland Groups, allowing overpressures to dissipate more rapidly.

The overpressures in the Schieland Group reservoirs in the Terschelling Basin do not show similar regional variations: the overpressures relative to the normal hydrostatic gradient all exceed 10 MPa and are comparable in magnitude with those observed in the L01 and L05 blocks (Figures 4.2.5, 4.2.6). The overpressures are likewise maintained by overlying low permeable claystones of the Schieland and Rijnland Groups, the Chalk Group and the Lower Tertiary claystones. Two local deviating relatively high overpressure values (> 12 MPa) were observed at wells G16-02 and M01-01; the Schieland reservoirs at both locations occur on top of a Zechstein salt structure.

Excess pressures in the Germanic Trias Group (hydrostratigraphic domains 3 and 4)

As described above, the most important low permeable units controlling the preservation of pressure in the Terschelling Basin and the southern part of the Central Graben are the Zechstein salt deposits and structures and the salt deposits of the Upper Germanic Trias Group (Röt Formation). The cross-sections (Figures 4.2.4, 4.2.5, 4.2.6) clearly show this influence. The highest overpressure values occur in those Lower Germanic Trias units that overlie the Zechstein salts, are capped by Triassic salts and are laterally hydraulically restricted by Zechstein salt structures and/or sealing faults (for example at well L05-07 in the Dutch Central Graben and well M01-02 in the Terschelling Basin).

Outside the areas that are hydraulically restricted by Zechstein and Triassic salts, the pore water in the Lower Germanic Trias is still overpressured, but less extreme, and overpressure values approach those observed in Upper Jurassic units (for example in the south eastern part of the Terschelling Basin, block M04, Figure 4.2.6).

Excess pressures in the Upper Rotliegend Group (hydrostratigraphic domain 1)

The fluid overpressure exceeding 40 MPa in the Upper Rotliegend Group in the southern part of the Central Graben clearly indicate that very high overpressures can be maintained below the Zechstein Group, where both vertical and lateral dewatering of the Upper Rotliegend Group is restricted. Southward of the Dutch Central Graben and the Terschelling Basin, the Upper Rotliegend sandstone reservoir units become more laterally continuous and also more hydraulically continuous, enabling lateral migration of the formation fluids and dissipation of overpressures. The fluid overpressures in the Upper Rotliegend units in the Friesland platform and the Central Offshore Platform rapidly reduce to values of 10 MPa and less (Figure 4.2.4).

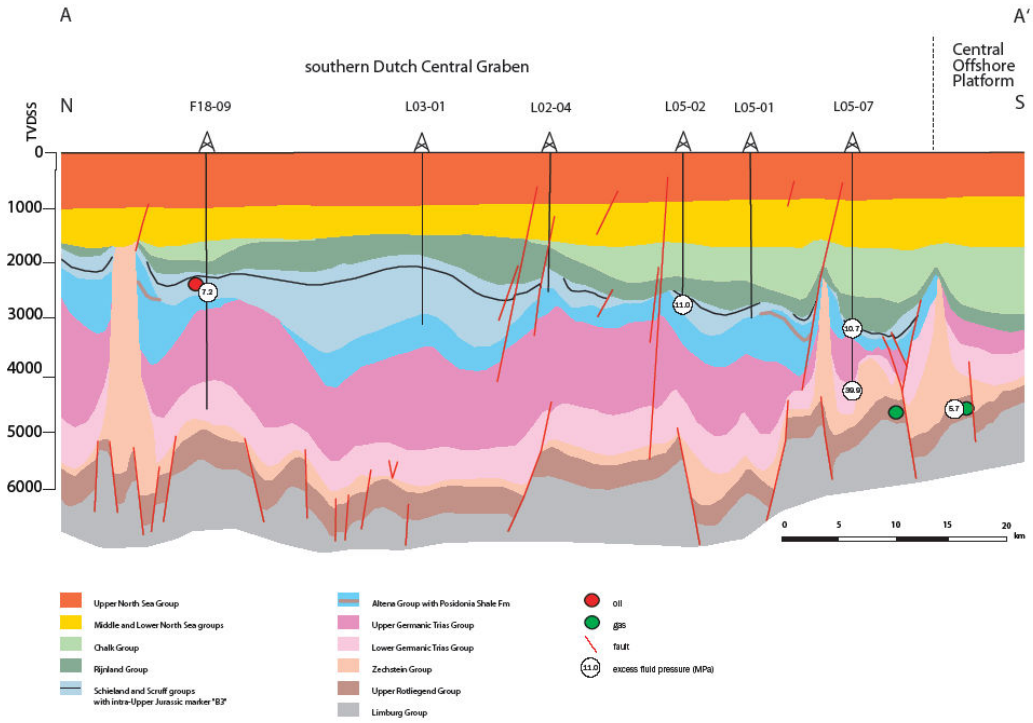

Figure 4.2.4 N-S cross section through the Dutch Central Graben showing regional distribution of pore fluid overpressures

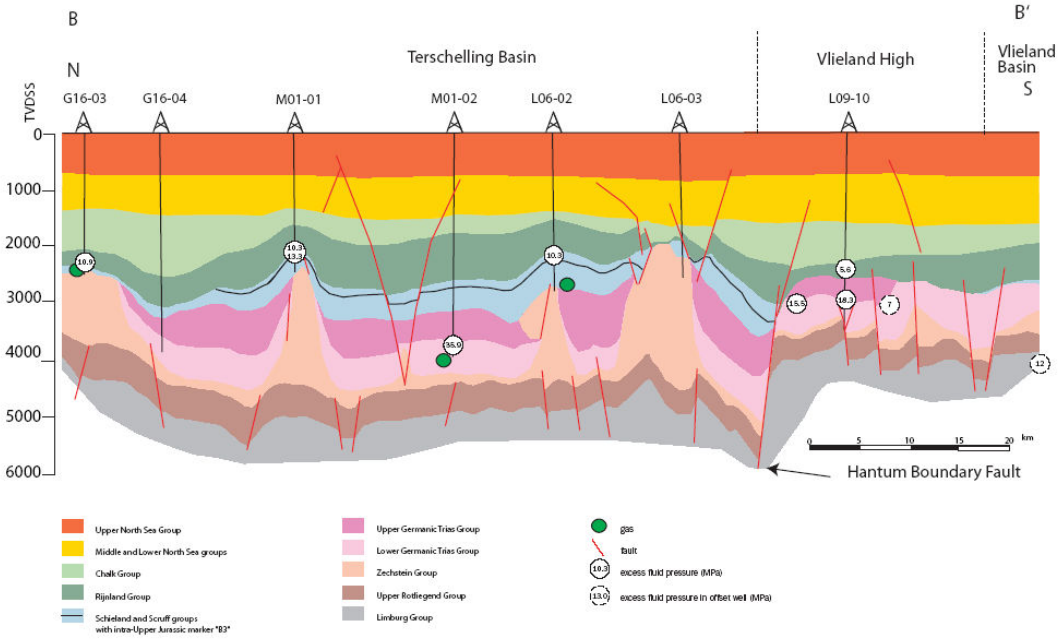

Figure 4.2.5 N-S cross section through the Terschelling Basin and Vlieland High showing regional distribution of pore fluid overpressures

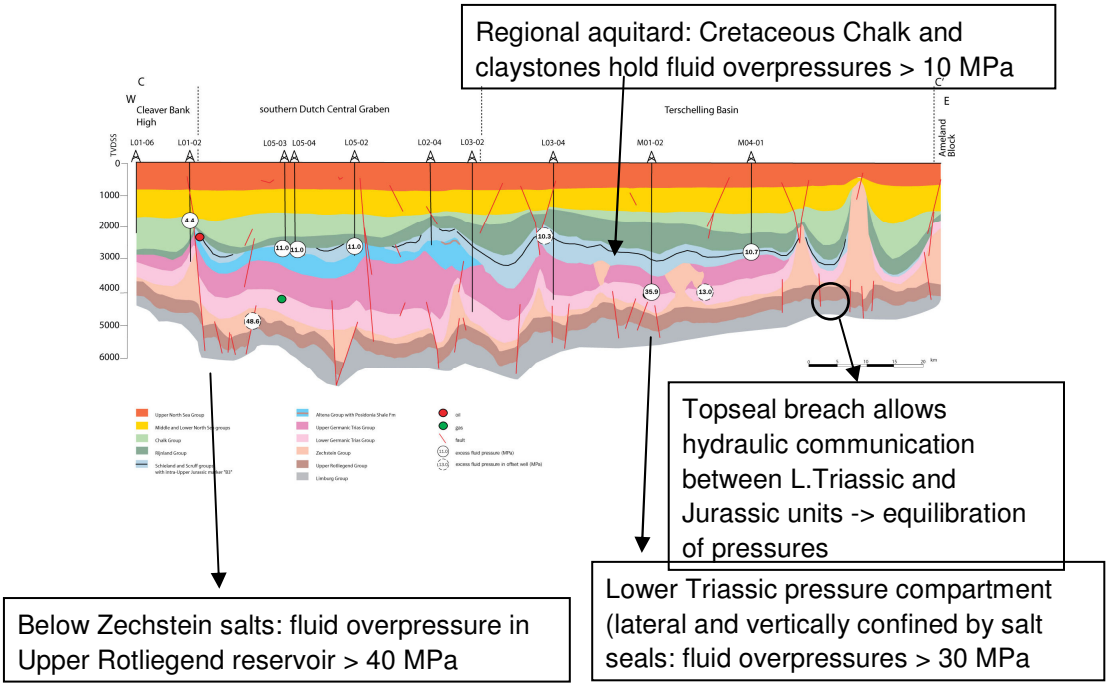

Figure 4.2.6 W-E cross section through the Dutch Central Graben and the Terschelling Basin showing regional distribution of pore fluid overpressures

4.3 Petroleum system

4.3.1 Source rocks

The main source rocks for gas are the coal measures of the Limburg Group. These source rocks of kerogen type III include the Baarlo Formation, Ruurlo and the Maurits Formation. The occurrence of the Maurits Formation is probably restricted to the southwestern part of the area. Coal layers in the Central Graben Subgroup (Schieland Group) are considered to be secondary source rocks for gas.

The Posidonia Shale Formation is the main source rock for oil. The present-day distribution of this type-II source rock is restricted to the southern part of the Dutch Central Graben. Possible additional source horizons occur in the Aalburg and Sleen Formations of the Altena Group (De Jager and Geluk 2007).

Table 4.3.1 Average source rock parameters measured at 22 wells in and around the study area

Source rock	TOC (wt%)average	HI (mgHC/gTOC
Posidonia	9	579.22
Maurits	4.43	194.84
Ruurlo	10.75	64.33
Baarlo**	5.98	91.30

**TOC and HI values derived from wells in southern part Dutch North Sea

4.3.2 Reservoirs

The mapping project aimed to increase the quantitative knowledge on the distribution, thickness and porosity of the lithostratigraphic units of reservoir quality in the southern part of the Dutch Central Graben and the Terschelling Basin. Annex L presents a map showing the distribution of gas and oil accumulations in the area. The proven reservoir units are summarised in Table 4.3.2.

The lateral continuity of the sandstone reservoir units of the Triassic groups and also those of the Schieland and Scruff Groups have been disrupted to a greater or lesser extent by the large Zechstein salt structures (see thicknesss and depth maps, Annexes B and C).

Benedictus (2007) calculated net porosity values from bulk density logs of the the Lower Volpriehausen and Detfurth Sandstone Members of the Lower Germanic Trias Group, the Upper Germanic Fat Sandstone Member and of several potential reservoir units of the Jurassic Schieland and Scruff groups. Annex J provides an overview of the calculated porosities).

Table 4.3.2 indicates that the Lower Slochteren Member of the Slochteren Formation is also a potential reservoir unit. However, there are no calculated porosities of reservoir units of the Upper Rotliegend Group available for the study area itself. Benedictus did calculate porosities for wells penetrating the Upper Rotliegend reservoirs southward of the study area (Annex J). Annex J Reveals that there are large lateral variations in porosity in all reservoir units in the studied area.

Information on measured reservoir permeabilities is limited and concerns the Triassic and Jurassic units only.

Table 4.3.2 Overview of proven and potential reservoir units in the studied area

Group	Proven reservoirs (for gas)	Additional reservoir-type lithostratigraphic units
Limburg Group (DC)		Hospital Ground (DCDG) and Step Graben Formation (DCHP); remnants encountered in SW part of area (Annex?)
Upper Rotliegend Group (RO)	Lower Slochteren Member (ROSLL); southernmost part of Dutch Central Graben and on Central Offshore Platform	
Zechstein Group (ZE)		Z1 Carbonates
Composite Zechstein/Schieland Groups	Composite Zechstein/Schieland Groups reservoir above salt structure, gas field G16-FA)	
Lower Germanic Trias Group	Sandstone units of Main Buntsandstein Subgroup RBM (such as Lower Volpriehausen Sandstone Member RBMVL); in Dutch Central Graben, Terschelling Basin, Friesland Platform, Vlieland Basin	Lower Detfurth Sandstone Member (RBMDL); RBMDL and RBMVL have their greatest thickness in the Graben (Annex?)
Upper Germanic Trias Group (RN)	Solling Fat Sandstone Member (RNSOF); block L09: Friesland Platform, Lauwerszee Trough	
Schieland and Scruff Groups (SL, SG)	Terschelling Sandstone Member (SLCFT); Block L06 in Terschelling Basin; Friese Front Formation* (SLCF); Dutch Central Graben	Scruff Greensand Formation (SGGS), Schill Grund Member; Annex? shows thickness Terschelling Sandstone Member
Chalk Group (CK)		Maastrichtian and Danian part Chalk Group
North Sea Group (N)		Quaternary sands (NU)

* proven reservoir for oil

Triassic reservoirs

Important Triassic reservoirs of great regional extent are the Lower Volpriehausen and Detfurth Sandstone Members. The thickness of the Lower Volpriehausen Sandstone Member increases from east to west from approximately 20 to 50 meters.

The porosity-depth plot (Figure 4.3.1) shows that there are large lateral variations of the porosity in all sandstone units of the Main Buntsandstein Subgroup. Previous studies have shown that the reservoir quality of sandy units of the Main Buntsandstein Subgroup in the southern Dutch Central Graben is affected by pore filling cements, such as dolomite, anhydrite and halite (Dronkert and Remmelts 1996; Purvis and Okkerman 1996). Purvis and Okkerman used petrographic and isotopic data to study the origin of the anhydrite and halite cements. They suggested that the most likely source for anhydrite and halite are the Zechstein Evaporites, although they do not rule out the Upper Triassic Rot salt as a possible source for the halites. Purvis and Okkerman's preferred interpretation involves anhydrite and halite cementation at relatively shallow burial depth. In general, brines from the Zechstein may be able to enter the Triassic reservoirs by lateral contact of the reservoirs with Zechstein structures, or by vertical flow through fault and fracture systems.

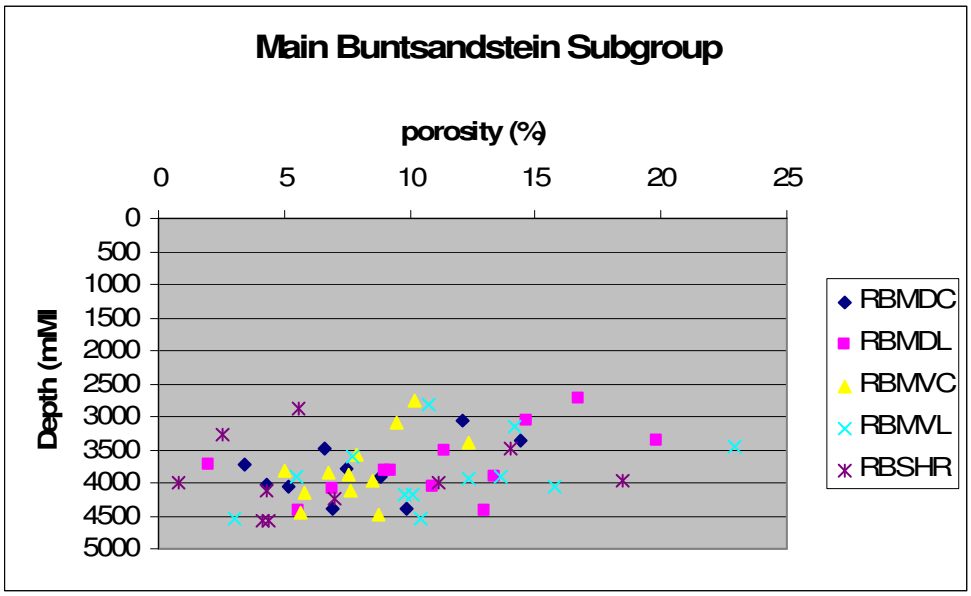

Figure 4.3.1 Porosity-depth plot of the different reservoir units in the Main Buntsandstein Subgroup

The porosity-depth plots for the Lower Volpriehausen Sandstone Member (Figure 4.3.2.) and the Lower Detfurth Sandstone Member (Figure 4.3.3.) suggest that the reservoir porosities are higher on the Cleaver Bank High and Friesland Platform in comparison with those observed in the basinal areas. Large lateral variations in porosity occur over relatively short distances in the Graben and the Terschelling Basin. For example in block L02: the porosity at a depth of 3500-4000 m at well L02-02 < 5.5% and at L02-07 > 13 %. Well L02-02 is located within a few hundred meters of a salt structure, and according to Dronkert and Remmelts (1996), the Lower Volpriehausen Sandstone Member shows salt plugging at this well location, in contrast to wells, located at more than 1.5 km from the salt structure (amongst other wells , L02-07), that do not show signs of halite cementation.

Figures 4.3.2 and 4.3.3 show that the reservoir porosities at well L03-02 are 3-6 %. These relatively low porosities and the location of this well northeast of a large salt wall are in accordance with a possible spatial relation between salt structures and low porosities due to salt plugging (in addition, a normal fault crosses the Upper Triassic in well L03-02).

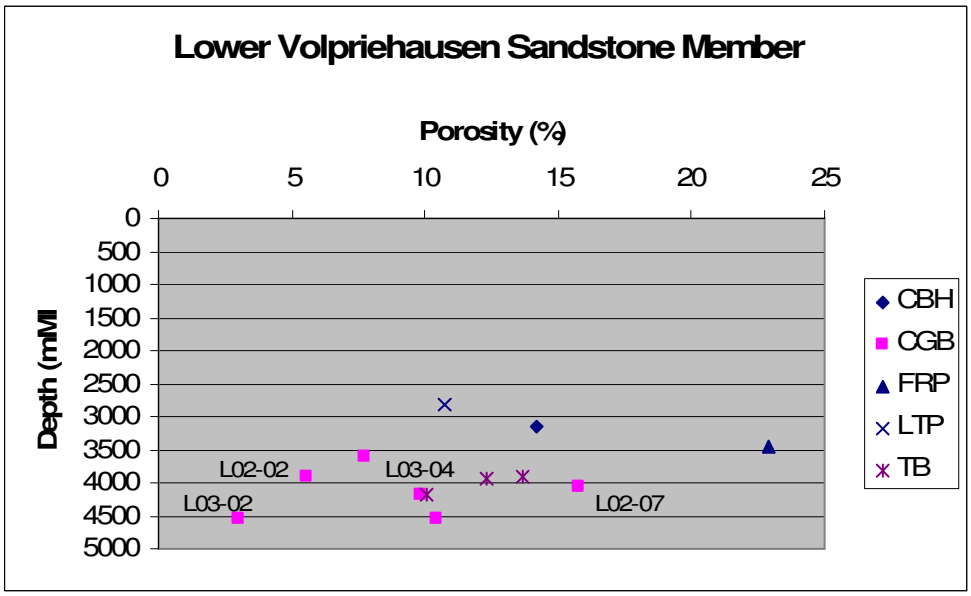

Figure 4.3.2. Porosity-depth plot of the Lower Volpriehausen Sandstone Member of the Main Buntsandstein Subgroup for different structural elements.

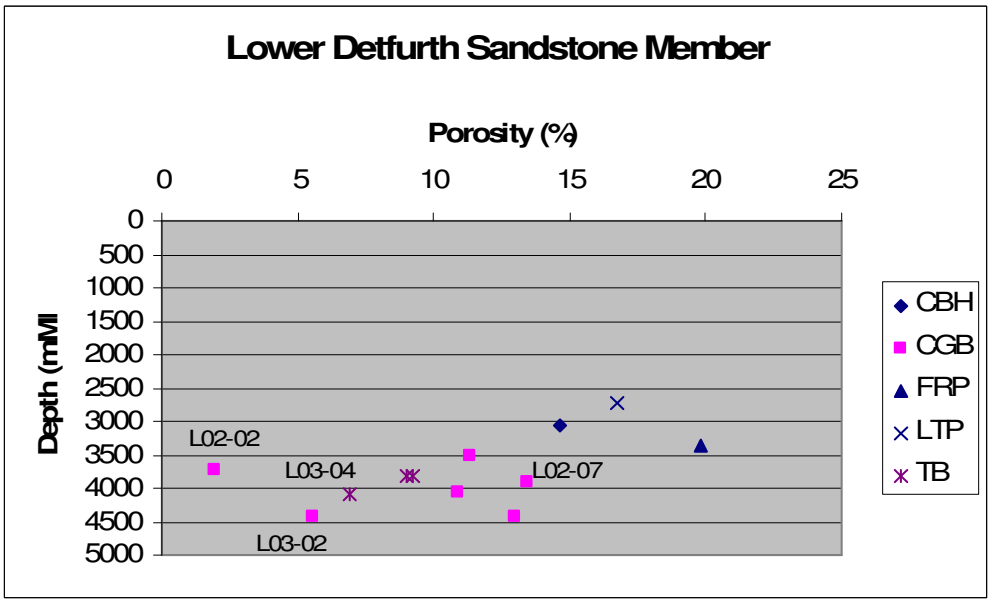

Figure 4.3.3 Porosity-depth plot of the Lower Detfurth Sandstone Member of the Main Buntsandstein Subgroup for different structural elements.

The measured average horizontal permeability of Triassic reservoirs is low and values vary between 1-7 mD for wells L02-02, -05 and also for L02-07 in the southern part of the Central Graben, and are about 1mD at well M01-01 in the Terschelling Basin.

The Solling Fat Sandstone Member is a proven reservoir in block L09. It reaches a thickness of 165 m, has a net overgross ratio of close to 100% and a porosity of 22 % (at well L09-10, Annex J), and the producing reservoir is characterised by average permeabilities in the Darcy range (De Jager and Geluk 2007). However, its distribution is restricted to blocks L09 and L06, and it has only been encountered locally in blocks L01 and F18. The porosity of the Solling Fat Sandstone member at wells L06-01 and L01-06 are greatly reduced (7 and 0.7 %, respectively; Annex J).

Upper Jurassic reservoirs

The plots of the mean net porosities versus depth for the reservoirs of the Schieland and Scruff Groups show a general decrease of porosity with depth (Figure 4.3.4). Scattering of porosity data starts already at depths of less than 2000 m.

Figure 4.3.4. Porosity-depth plot of the reservoir units of the Schieland and Scruff Groups

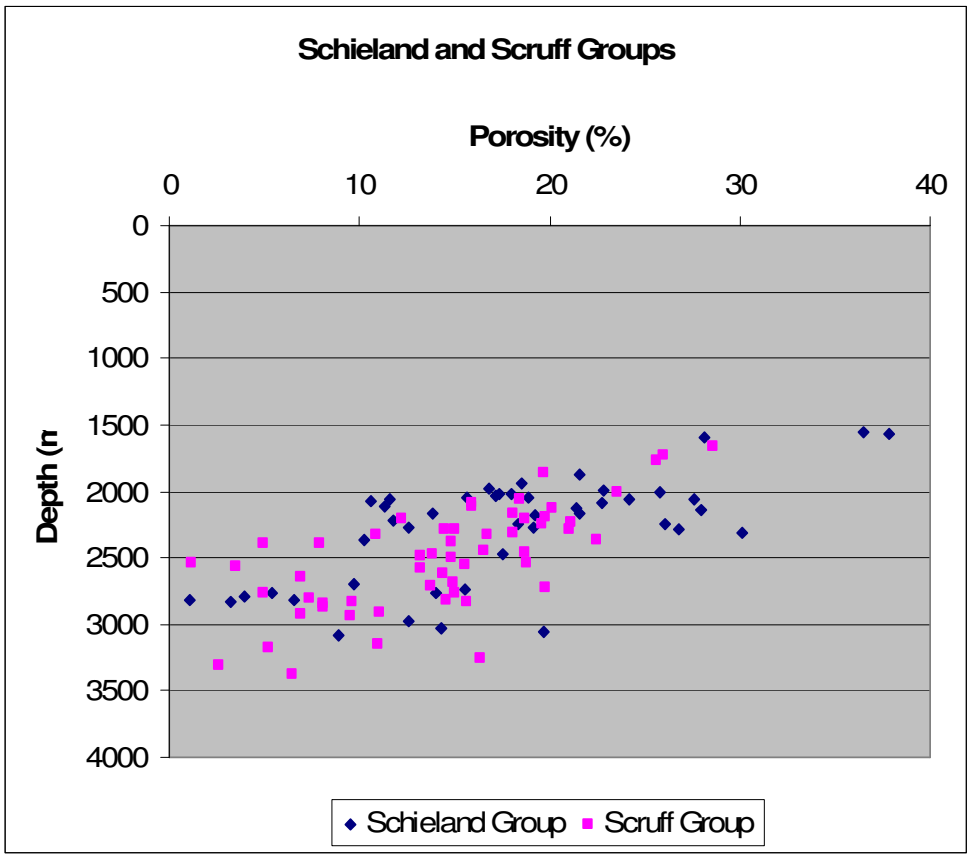

Figure 4.3.5 shows the lateral variation of the porosity of the Schieland Group reservoirs. For example, the mean net porosity of the reservoir units in the Schieland Group at wells L06-02 and M01-01 are already greatly reduced to 13% at at depths of approximately 2100 m, while the porosities at wells F18-01 and F18-02 are around 24 %. The Schieland Group at wells L06-02 and M01-01 directly overlies Zechstein salt structures. It has not been investigated whether or not the Schieland Group reservoirs are salt plugged at these locations.

The porosity of the reservoir units in the Schieland and Scruff groups encountered at well L02-02 varies between 20 – 28% at depth between 2000-2400 m. It is interesting to note the difference between these relatively good porosities in the Jurassic reservoirs in contrast to the reduced porosities by salt plugging observed in the Triassic reservoirs in the same well. The close location of well L02-02 to the salt structure did not seem to have influenced the porosities of the Jurassic reservoirs.

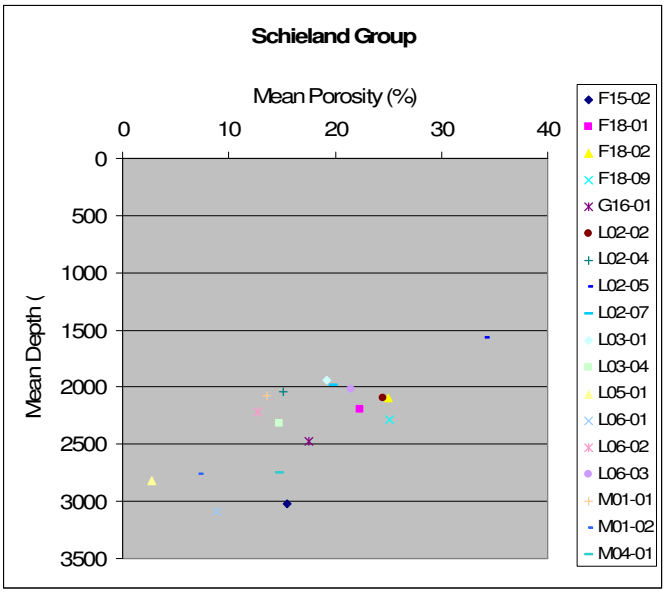

Figure 4.3.5 Porosity-depth plot of the mean net porosities of the reservoir units of the Schieland Group sorted by well location.

The measured average horizontal permeability in the Schieland reservoir units is 400-600 mD (SLCFT and SLCF in wells L03-01, L06-02 and L06-03)

4.3.3 Oil and gas characteristics

The characterisation of the natural oil and gas in the Terschelling Basin and the southern Dutch Central Graben is based on analysis and interpretation of information from the non-confidential database on the composition of natural gas and - for oil - on information from stranded fields. Annex L displays the regional variation of selected calculated gross heating values of hydrocarbon gases and the variation for the molecular ratio of CH_4 and total gas content in gas accumulations in the study area. The map also provides information on the API gravity of the oil accumulations.

Composition of natural gas

The gas composition data show that the proportion of methane in the natural gases varies between 72 and 94 Mol%. A low proportion of methane could be related to two main causes: 1) a high proportion of non-hydrocarbons 2) or a high proportion of C2+ components, for example a low proportion of methane in L09-04 (74 Mol%) is associated with a high proportion of nitrogen (>20 Mol%), while in F17-04 (75Mol% methane) it is due to a high proportion of C2+ components (20 Mol%).

The gas database includes 16 analyses of the carbon and hydrogen isotopic composition of methane. The relation between the carbon and hydrogen isotopic composition of methane is plotted in Figure 4.3.6. The range of values correspond with dry thermogenic gas, and - to a minor extent - with thermogenic gas with condensate.

The calculated gross heating values of the hydrocarbon gases range between 33 (observed in well L09-04) and 52 MJ/m^3. Values exceeding $45MJ/m^3$ occur in gases encountered in Fields F17-FA and F17-FB. These gases, associated with the oil fields F17-FA and-FB, contain a relatively high proportion of C2+ components (14 and 20 Mol% in well F17-03 and F17-04, respectively).

Non-hydrocarbon gases

Nitrogen is the most abundant non-hydrocarbon gas component encountered. The nitrogen content varies between 0.8 and 20.8 Mol%. The isotopic composition of nitrogen shows values of $\delta^{15}N$ ranging from -4.7 to 11.5 ‰ (based on 11 analyses of gas samples). The most enriched gas was encountered in well G16-03 in the Terschelling Basin (Figure 4.3.7 and 4.3.8).

The CO_2 content varies between 0 and 7.3 Mol%. Figure 4.3.9 shows that the CO_2 content of the gas accumulations in the Upper Rotliegend reservoirs is high compared with the content encountered in gas accumulations in Triassic and Jurassic reservoir units. The isotopic characteristics of the CO_2 in the gas accumulations are visualised in the cross-plots of $d^{13}C$-CO_2 versus the Mol% of CO_2 per structural unit (Figure 4.3.10). The carbon stable isotopes of CO_2 in the gas range between -8.0 and -5.3 ‰ PDB. This range of values suggest a possibly mixed organic and inorganic origin of the CO_2.

The gas samples included in the gas database contain no H_2S, suggesting the presence of H_2S is below detection limits in the mapped area.

A comprehensive overview of the main factors and processes of influence on the present-day non-hydrocarbon composition of natural gas accumulations in onshore and offshore Netherlands (Verweij 2006b) is available at www.nlog.nl.

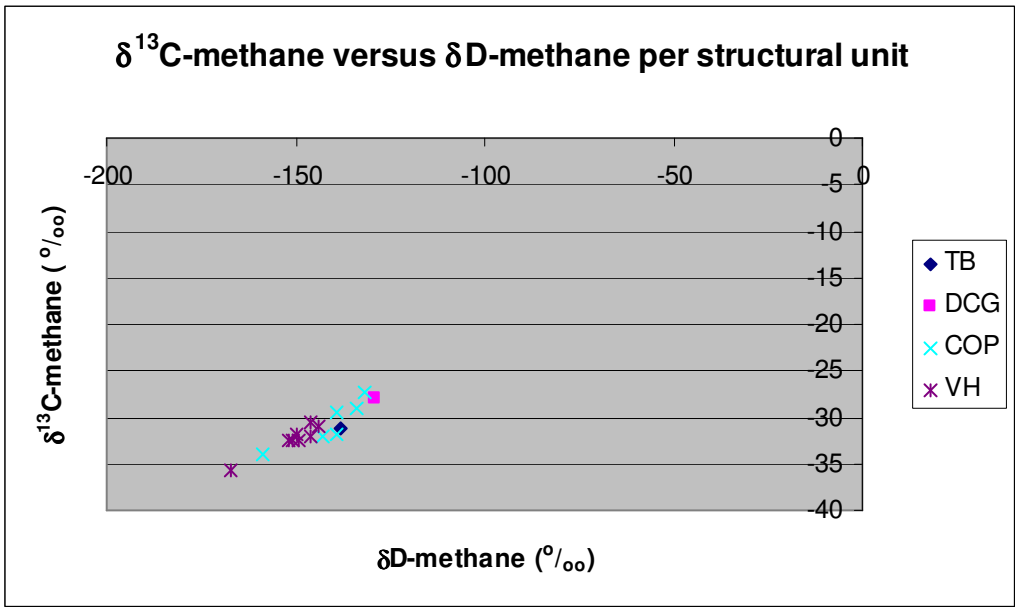

Figure 4.3.6. Cross-plot of the carbon and hydrogen isotopic composition of methane. According to the Schoell (1983) classification the gases with δD methane >150 ‰ correspond to dry thermogenic gases, and gases with δD methane <150 ‰ are thermogenic gases with condensate.

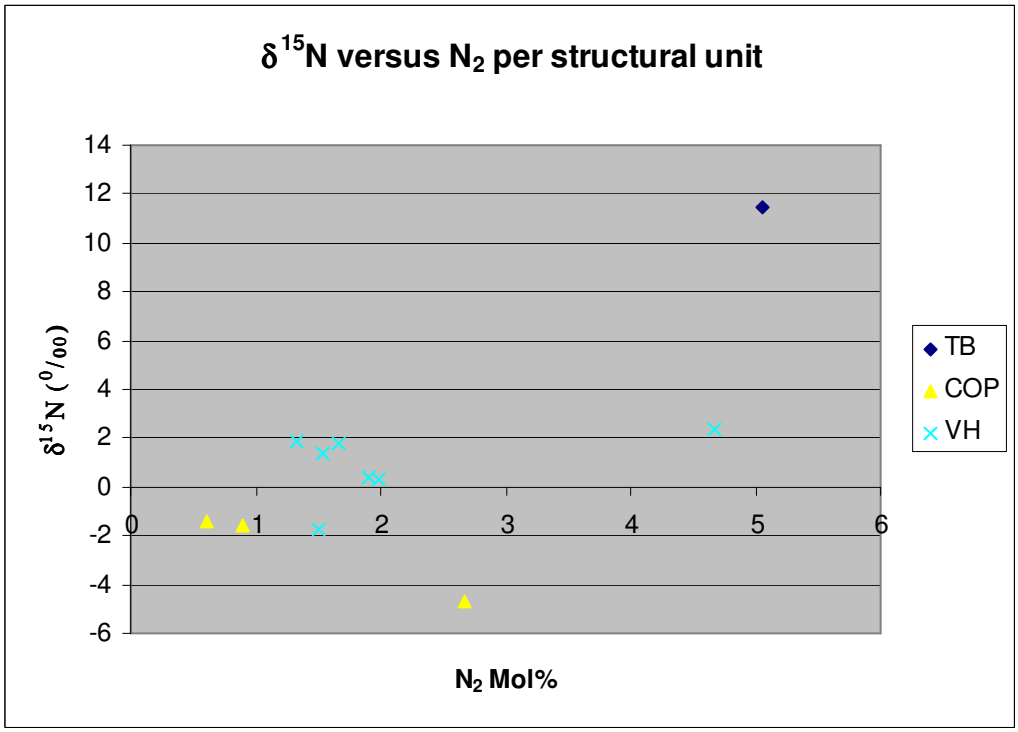

Figure 4.3.7 Cross plot of values of d15N versus nitrogen content in natural gas accumulations grouped per structural element.

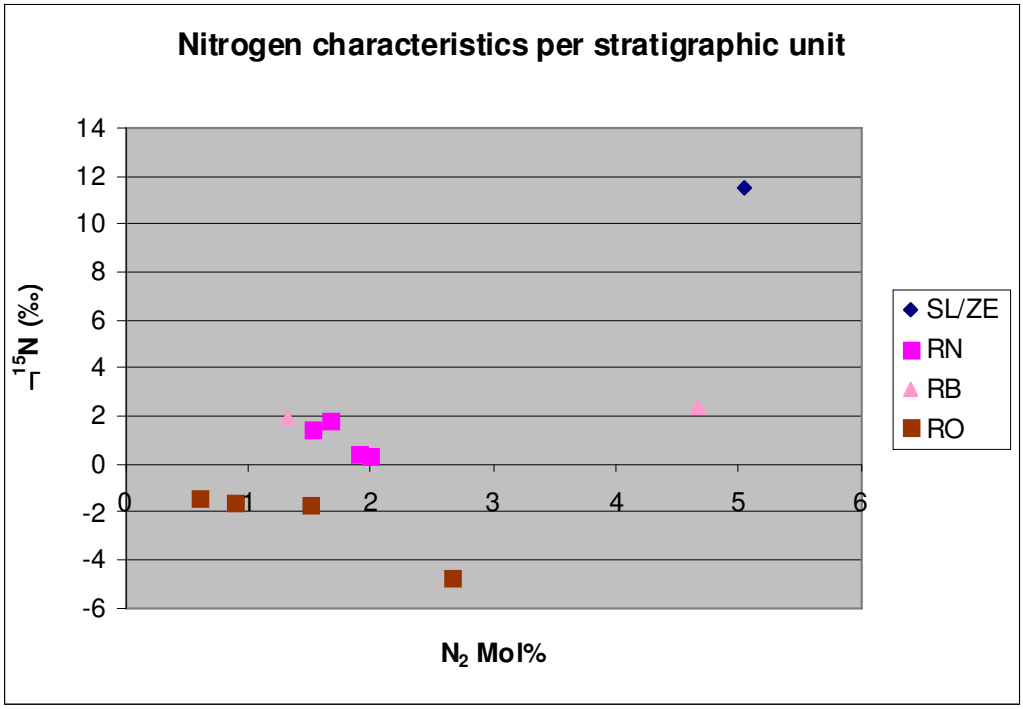

Figure 4.3.8 Cross plot of values of d15N versus nitrogen content in natural gas accumulations grouped per stratigraphic unit.

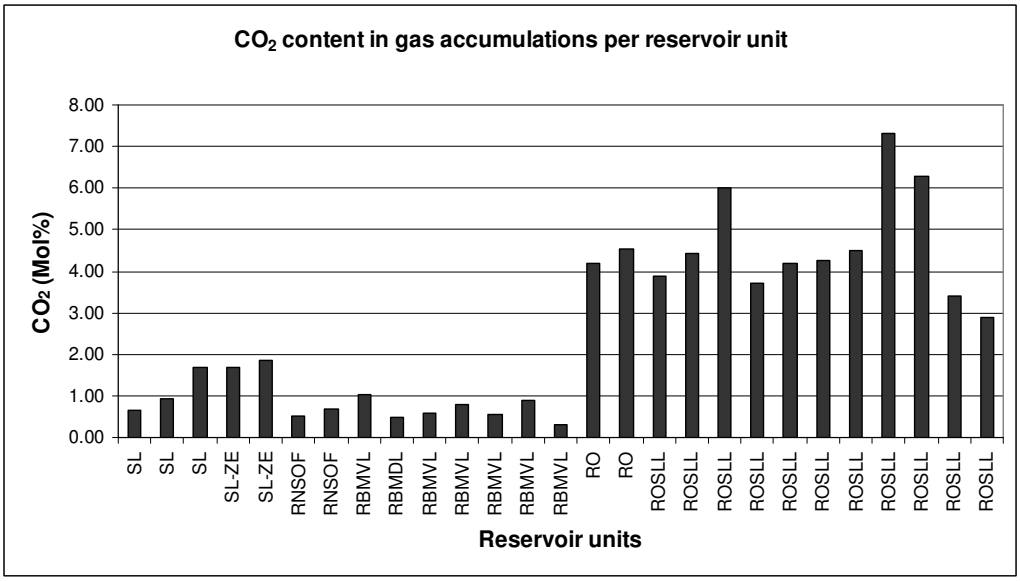

Figure 4.3.9 Cross plot of the CO_2 content in natural gas accumulations per reservoir unit. The gas accumulations in the Rotliegend reservoirs contain higher percentages of CO_2 than the gases reservoired in post-Zechstein units.

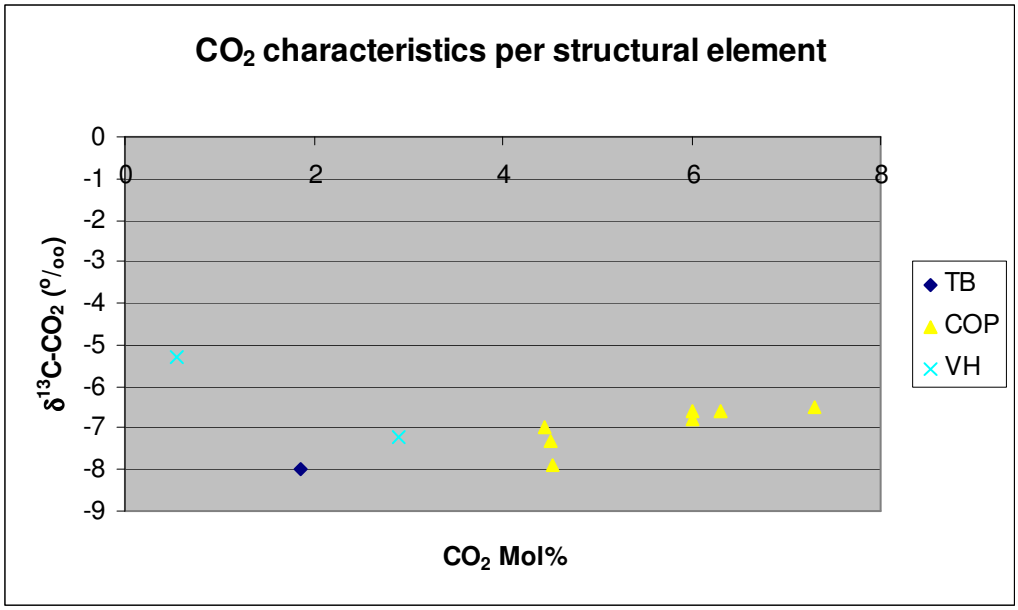

Figure 4.3.10 Cross plot of values of $\delta^{13}C$ of CO_2 (PDB) versus CO_2 content (Mol ‰) in natural gas accumulations per structural element.

4.4 Geothermal conditions

The temperature-depth plot (Figure 4.4.1) shows the temperature measurements from different sources and of different reliability in the Terschelling Basin and southern Dutch Central Graben. These temperature measurements were used to calculate geothermal gradients at each well, applying a Bayesian statistical method and assuming a surface temperature of 9 ^{o}C. The multi-well geothermal gradient for the entire study area is relatively high: 34 ^{0}C/km. Annex N shows the geothermal gradients that were calculated for the post-Zechstein sedimentary sequence.

The variations in bulk thermal conductivity of the subsurface have a major influence on the lateral and vertical temperature distribution and the related variations in geothermal gradients. Salt (halite) has a temperature dependent thermal conductivity of 5.4 $Wm^{-1}K^{-1}$ at 20^{o}C to 3.2 $Wm^{-1}K^{-1}$ at 160^{o}C, which is significantly higher than clastic lithologies. The greatly varying thicknesses of the Zechstein Group cause strong lateral variations in bulk thermal conductivities.

The geothermal gradients map (Annex N) shows that the gradient varies laterally between 30 and 46^{o}C/km in post-Zechstein sediments. The occurrence of geothermal gradients with values of ≥40^{o}C coincides with measurements on top of salt structures (for example, at wells M01-01, L06-02, G16-03 and L05-06). The rapid transfer of heat through the salt diapirs produces positive temperature anomalies in the sediments overlying the salt structure. This effect seems to be most pronounced on top of the very thick salt diapir (3760 m) that reaches shallow depths (640m) at well L05-06.

The calculated geothermal gradient on top of the salt diapir at well L05-06 is 46 °C/km. This well penetrates the entire salt diapir and measured temperatures below the salt are relatively low. This negative temperature anomaly is reflected in the low geothermal gradient, 22°C/km, calculated for the interval between the ground surface temperature and the measured sub-salt temperatures.

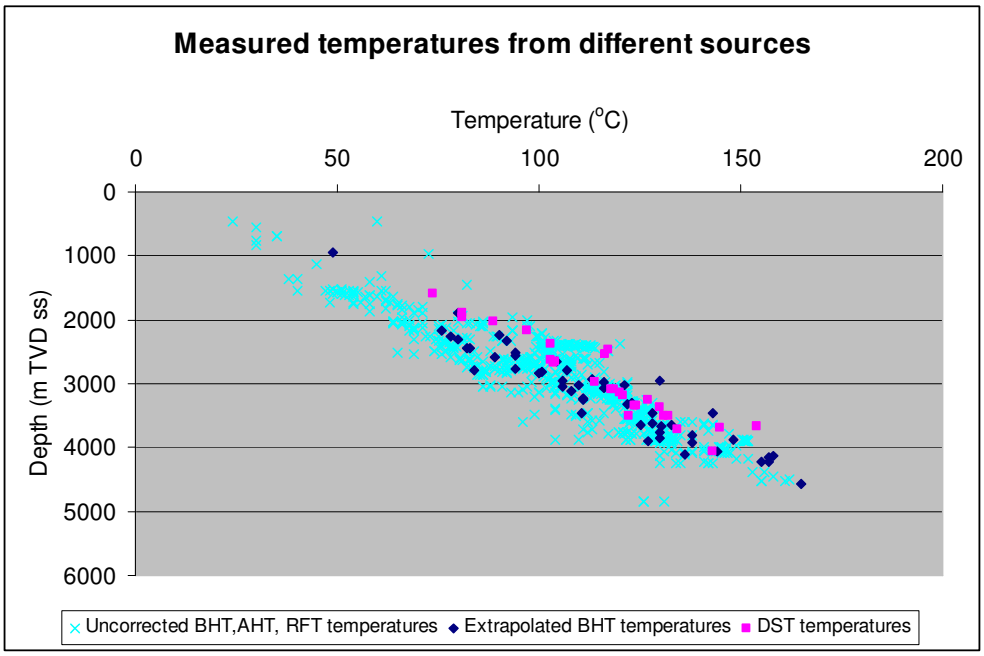

Figure 4.4.1 Temperature measurements in the Terschelling Basin and the southern Dutch Central Graben. Most temperatures were measured at depths between 1500 and 4500 m. Note the large variation in temperatures at the same depth of measurement. The DST temperatures are considered to be the most reliable temperatures and most representative of the virgin rock temperatures.

5 References

Abbink O.A., Mijnlieff H.F., Munsterman D.K. & Verreussel R.M.C.H. New stratigraphic insights in the 'Late Jurassic' of the Southern Central North Sea Graben and Terschelling Basin (Dutch Offshore) and related exploration potential. Netherlands Journal of Geosciences — Geologie en Mijnbouw, 85-3, p. 221-238.

Alblas, L.D. (2001) The petroleum industry in the Netherlands – its settings and possible future. Geol. Mijnbouw/Neth. Journ. Geosc. 80, p. 23-32.

Breunese, J.N. & Rispens, F.B. (1996) Natural gas in the Netherlands: exploration and development in historic and future perspective. In: Rondeel, H.E., Batjes, D.A.J. & Nieuwenhuijs, W.H. (eds) Geology of Gas and Oil under the Netherlands. Kluwer, Dordrecht, p. 19-30.

De Jager, J., Doyle, M.A., Grantham, P.J. & Mabillard, J.E. (1996) Hydrocarbon habitat of the West Netherlands Basin. In: Rondeel, H.E., Batjes, D.A.J. & Nieuwenhuijs, W.H. (eds) Geology of Gas and Oil under the Netherlands. Kluwer, Dordrecht, p. 191-209.

De Jager, J., 2003. Inverted basins in the Netherlands, similarities and differences. Netherlands Journal of Geosciences / Geologie en Mijnbouw 82: p. 339-349.

De Jager, J., 2007. Geological Development. In: Wong, Th.E, Batjes, D.A.J. & De Jager, J. (eds): Geology of the Netherlands. Royal Netherlands Academy of Arts and Sciences (Amsterdam): p. 5 -26.

De Jager, J. & Geluk, M.C., 2007. Petroleum Geology. In: Wong, Th.E., Batjes, D.A.J. & De Jager, J. (eds): Geology of the Netherlands. Royal Dutch Academy of Arts and Sciences (Amsterdam): p. 241 -264.

Dirkzwager. J.B., 2002. Tectonic modelingof vertical motion and its near surface expression in the Netherlands, PhD thesis, VU-Amsterdam: 156 pp.

Dronkert, H. and Remmelts, G. 1996. Influence of salt structures on reservoir rocks in Block L2, Dutch continental shelf. In: Rondeel, H.E., Batjes, D.A.J. & Nieuwenhuijs, W.H. (eds): Geology of gas and oil under the Netherlands. Kluwer (Dordrecht), 179-189.

Duin E.J.T., Doornenbal J.C., Rijkers R.H.B., Verbeek J.W.& Wong Th.E., 2006. Subsurface structure of the Netherlands - results of recent onshore and offshore mapping, Netherlands Journal of Geosciences - Geologie en Mijnbouw, 85-4, pp. 245 - 276.

Frikken, H.W. (1999) Reservoir-geological aspects of productivity and connectivity of gasfields in the Netherlands. PhD thesis, Technical University Delft, 13/9/99, 91 pp.

Geluk, M.C. (1999a) Late Permian (Zechstein) rifting in the Netherlands - models and implications for petroleum geology. Petroleum Geoscience 5 (2), p. 189-199.

Geluk, M.C., 2005. Stratigraphy and tectonics of Permo-Triassic basins in the Netherlands and surrounding areas. PhD thesis, University of Utrecht: 171 pp.

Geluk, M.C., 2007a. Permian. In: Wong, Th.E., Batjes, D.A.J. & De Jager, J. (eds): Geology of the Netherlands. Royal Dutch Academy of Arts and Sciences (Amsterdam): p. 63 - 83.

Geluk, M.C., 2007b. Triassic. In: Wong, Th.E., Batjes, D.A.J. & De Jager, J. (eds): Geology of the Netherlands. Royal Dutch Academy of Arts and Sciences (Amsterdam): p. 84 - 106.

Geluk, M.C., Paar, W.A. & Fokker, P.A., 2007 . Salt. In: Wong, Th.E., Batjes, D.A.J. & De Jager, J. (eds):: Geology of the Netherlands. Royal Dutch Academy of Arts and Science (Amsterdam): p. 283 – 294.

Gradstein, F.M., Ogg, J.G. & Smith, A.G. (eds), 2004. A geologic time scale. Cambridge University Press: 589 pp.

Herngreen, G.F.W. & Wong, Th.E., 1989. Revision of the 'Late Jurassic' stratigraphy of the Dutch Central Graben. Geologie en Mijnbouw 68: p. 73-105.

Herngreen, G.F.W., Smit, R. & Wong, Th.E., 1991. Stratigraphy and tectonics of the Vlieland Basin, The Netherlands. In: A.M. Spencer (ed.): Generation, accumulation and production of Europe's hydrocarbons. Special publications EAPG no. 1, Oxford University Press (Oxford): p.175-192.

Heybroek, P., 1974. Explanation to tectonic maps of the Netherlands. Geologie en Mijnbouw 53: p. 43-50.

Kuhlmann, G., 2004. High resolution stratigraphy and paleoenvironmental changes in the southern North Sea during the Neogene: An integrated study of Late Cenozoic marine deposits from the northern part of the Dutch offshore area – PhD Thesis, University Utrecht: 205 pp.

Netherlands Institute of Applied Geoscience TNO – National Geological Survey (2004). Geological Atlas of the Subsurface of the Netherlands – onshore, TNO – NITG, Utrecht: 101 pp.

Overeem, I., Weltje G. J., Bishop-Kay C.and Kroonenberg S. B. (2001) - The Late Cenozoic Eridanos delta system in the Southern North Sea Basin: a climate signal in sediment supply? Basin Research 13, p. 293-312.

Purvis, K. and Okkerman, J.A. 1996. Inversion of reservoir quality by early diagenesis: an example from the Triassic Buntsandstein, offshore the Netherlands. In: Rondeel, H.E., Batjes, D.A.J. & Nieuwenhuijs, W.H. (eds): Geology of gas and oil under the Netherlands. Kluwer (Dordrecht), 179-189.

Remmelts, G., 1996. Salt tectonics in the southern North Sea, the Netherlands. In: Rondeel, H.E., Batjes, D.A.J. & Nieuwenhuijs, W.H. (eds): Geology of gas and oil under the Netherlands. Kluwer (Dordrecht): 143-158.

Rijkers, R.H.B. & Duin, E.J.Th.,1994. Crustal observations beneath the southern North Sea and their tectonic and geological implications, Tectonophysics 240: p. 215-224.

Rijkers, R.H.B. & Geluk, M.C., 1996. Sedimentary and structural history of the Texel-IJsselmeer High, The Netherlands. In: Rondeel, H.E., Batjes, D.A.J. & Nieuwenhuis, W.H. (eds): Geology of gas and oil under the Netherlands. Kluwer (Dordrecht): p. 265-284.

Van Adrichem Boogaert, H.A. & Kouwe, W.F.P. (eds), 1993 - 1997. Stratigraphic nomenclature of the Netherlands, revision and update by RGD and NOGEPA, Mededelingen Rijks Geologische Dienst 50.

Van Dalfsen, W., Doornenbal, J.C., Dortland, S. & Gunnink, J.L. (2006). A comprehensive seismic velocity model for the Netherlands based on lithostratigraphic layers, Netherlands Journal of Geosciences / Geologie en Mijnbouw 85/4: p. 277-292.

Van der Molen, A.S., 2004. Sedimentary development, seismic stratigraphy and burial compaction of the Chalk Group in the Netherlands North Sea area, PhD thesis. University Utrecht: 175 pp.

Van Wijhe, D.H., 1987. Structural evolution of inverted basins in the Dutch offshore. Tectonophysics 137: p. 171-219.

Verweij, J.M. (2003) Fluid flow systems analysis on geological timescales in onshore and offshore Netherlands. With special reference to the Broad Fourteens Basin. Doctoral Thesis Vrije Universiteit Amsterdam, 278 pp.

Wong, Th.E., Batjes, D.A.J. & De Jager J. (eds), 2007. Geology of the Netherlands, Royal Netherlands Academy of Arts and Sciences (Amsterdam) 354 pp.

Ziegler, P.A., 1988. Evolution of the Arctic-North Atlantic and the Western Tethys, American Association of Petroleum Geologist Memoir 43: p. 164-196.

Ziegler, P.A., 1990. Geological Atlas of Western and Central Europe (2nd edition). Shell Internationale Petroleum Maatschappij B.V.; Geological Society Publishing House (Bath): 239 pp.

Internal TNO reports:

Internal TNO reports and reports by interns and trainees are made available upon request.

Abdul Fattah, R. (trainee, 2007-2008), Van Wees, J-D., Verweij, J.M., Bonte, D. 2008. Tectonic heat flow modelingfor the NCP2a area of the Dutch offshore. TNO report 2008-U-R0558/A

Benedictus, T (trainee, 2007). Determination of petrophysical properties from well logs of the offshore Terschelling Basin and southern Dutch Central Graben region (NCP-2A) of the Netherlands. TNO report 2007-U-R0169/A.

Stegers, D.P.M. (intern, 2006). Sedimentary facies analysis of sequence 2 of the Upper Jurassic in the Terschelling Basin and the southern Dutch Central Graben. TNO report 2006-U-R0191/A.

NITG-TNO (1997). Resultaten van het palynologisch onderzoek van boring L09-02, kerntraject 2929-2957 m. TNO report NITG 97-119-C.

NITG-TNO (1997). De resultaten van het palynologisch onderzoek naar de ouderdom en het afzettingsmilieu van de Friese Front Formatie ioin bnoringg L/3-01, traject: 2429-2842 m. TNO report NITG-97-16-B.

TNO BenO (2005). De resultaten van het dinoflagellaatcystenonderzoek naar de oudendom van boring M05-01, interval 1949-1976 m. Een palynologische studie naar de vertegenwoordiging van de Scruff Groep. TNO report NITG 05-129-B.

TNO BenO (2005). Carboniferous palynostratigraphy of Wells M03-01 and M10-04; NCP-2a. TNO report NITG 05-130-B0905.

TNO BenO (2005). De resultaten van het palynologisch onderzoek naar het Tertiair van boring L06-02 (interval: 230-1450 m) en L06-03 (interval: 200-1620 m). TNO report NITG 05-124-B.

TNO BenO (2007). Biostratigraphy of the upper Chalk Group; well L03-02, offshore the Netherlands. TNO report 2007-U-R0671/B.

Verweij, J.M., Souto Carneiro Echternach, M., Witmans, N. 2009. Terschelling Basin and southern Dutch Central Graben Burial history, temperature, source rock maturity and hydrocarbon generation - Area 2A. TNO report 2009-U-R (in prep)

6 Appendices

6.1 List of wells

SHORT_NAME	UTM3_X	UTM3_Y	TD	OPERATOR	END_DATE
F14-06	599797	6006768	2296	STA	03/09/1987
F14-06-S1	599797	6006768	2020	STA	04/10/1987
F15-01	626477	6020895	3385	TEN	06/08/1976
F15-02	620298	6011757	3958	PET	05/10/1981
F17-01	599831	6000913	3875	NAM	14/04/1975
F17-03	597324	5991546	2200	NAM	10/05/1982
F17-04	594058	5991405	2624	NAM	06/08/1982
F17-05	599207	5991079	2335	NAM	22/12/1982
F17-07	595931	5991153	2300	NAM	04/08/1984
F18-01	613934	5996010	3746	TEN	06/06/1970
F18-02	613213	5993234	2845	TEN	04/02/1971
F18-03	627672	5992753	2962	TEN	26/03/1972
F18-04	613367	5997172	3147	TEN	14/11/1972
F18-05	613417	5994541	2776	AGI	20/01/1981
F18-08	630059	5995711	3504	PEN	09/04/1986
F18-09	614885	5996503	4614	NAM	29/05/1987
G16-01	644089	5999997	4321	NAM	04/04/1985
G16-02	637907	5993588	3030	CON	09/04/1985
G16-03	643425	5999335	2850	NAM	14/11/1990
G16-04	641719	5993261	3925	CON	15/09/1991
G17-01	664316	5994909	3955	RFD	07/07/1969
G17-02	666835	6001586	4391	MOB	14/02/1985
G17-03	654844	5993199	3940	HAM	13/08/1992
G18-01	694010	5989188	4127	NAM	23/06/1983
L01-01	574952	5977915	3290	Unocal	15/02/1984
L01-02	580248	5973209	3070	Wintershall	07/06/1984
L01-04-A	567892	5967049	3953	CHH	15/10/1985
L01-06	572549	5974558	4459	Unocal	17/11/1986
L02-01	599291	5979580	4552	NAM	31/12/1968
L02-02	603393	5977115	4130	NAM	29/07/1969
L02-03	601040	5983018	2150	NAM	05/01/1971
L02-04	608515	5968908	2190	NAM	26/07/1971
L02-05	601490	5984002	4257	NAM	16/11/1976
L02-07	597892	5980020	4185	NAM	14/11/1982
L03-01	609785	5979241	3035	NAM	04/09/1971
L03-02	614403	5968751	4610	NAM	11/09/1991
L03-04	626102	5967996	4252	MOB	12/01/1993
L04-01	570877	5956460	3991	PET	31/08/1974
L04-03	567477	5953668	3830	PET	21/02/1981
L04-05	583843	5960544	4155	NAM	30/05/1992
L05-01	600848	5956048	3061	NAM	07/07/1975
L05-02	600455	5961490	2860	NAM	15/11/1979
L05-03	590964	5964826	2815	NAM	05/11/1983

L05-04	592412	5964372	2872	NAM	20/05/1985
L05-05	588797	5963250	4228	NAM	13/11/1988
L05-06	591537	5951583	4896	AMC	17/12/1991
L05-07	609240	5953395	4293	MOB	30/03/1993
L06-01	615427	5948889	4044	NAM	28/12/1989
L06-02	630946	5964891	2858	NAM	23/09/1990
L06-03	625751	5955898	2495	NAM	04/09/1991
L07-04	579792	5942872	4182	PET	23/12/1973
L08-02	594273	5935702	4307	PEN	30/12/1973
L08-03	597701	5942833	4429	PEN	21/03/1974
L08-07	589790	5945954	4700	AMC	25/08/1985
L08-P-01	603398	5944828	4836	WIN	13/06/1994
L09-01	614266	5935406	3825	PHL	22/06/1973
L09-02	616188	5945415	3085	NAM	12/03/1984
L09-04-S1	613848	5947808	4769	STA	22/02/1989
L09-06	624581	5937249	4442	NAM	07/04/1991
L09-07	629872	5939568	3530	NAM	02/08/1992
L09-10	629713	5942688	3512	NAM	29/03/1994
L09-11	629872	5939568	3483	NAM	13/12/1994
L12-01-A	617691	5915850	3451	SIG	20/01/1969
L12-02	617306	5911682	3276	NAM	02/05/1976
L12-03	623808	5913999	3150	NAM	11/07/1979
L12-04	621158	5914845	3171	NAM	02/03/1983
L12-05	620615	5927230	3708	NAM	01/02/1988
L15-01	624602	5908457	3202	NAM	16/07/1978
M01-01	640979	5982314	2527	NAM	19/09/1991
M01-02	637559	5969609	4004	NAM	21/03/1993
M03-01	687366	5973606	4500	BOW	24/12/1991
M04-01	642618	5953491	3015	Wintershall	24/06/1990
M04-03	637614	5956613	3841	Wintershall	04/01/1995
M05-01	675559	5957008	2007	CON	07/04/1986
M07-01	648815	5936965	3590	PHL	06/01/1969
M07-02	639921	5944199	3658	PET	24/10/1982
M07-03	641930	5947383	3010	PET	19/01/1984
M08-01	671888	5933324	3936	NAM	29/07/1982
M09-01	679966	5943649	3587	NAM	01/08/1968
M10-02	638409	5918069	3070	NAM	31/01/1982
M10-04	634425	5922385	3872	PLA	15/12/1988
M11-01	656900	5928249	3542	NAM	09/05/1982
N07-02	700179	5933279	3750	PLA	12/05/1991

6.2 List of seismic surveys

Blok	Survey code TNO
F17/F18	Z3NAM1992A
G16	Z3NAM1993C
L02	Z3NAM1991E
L03	Z3NAM1994B
L04/L05	Z3NAM1990B
L06	Z3NAM1990F
L09	Z3NAM1990G
M01	Z3NAM1990E
M02	Z3NAM1991A
M04	Z3NAM1991D
M05	Z3PET1991E
M07	Z3NAM1994A

6.3 List of maps (download page)

Southern Dutch Central Graben and Terschelling Basin (NCP-2A)

General data

Location of the offshore mapping areas
PDF

Location map of 3D seismic surveys and wells used
PDF

Structural setting

Structural elements map
PDF

Location of the cross sections
PDF

Cross section A - A'
PDF

Cross section B - B'
PDF

Cross section C - C'
PDF

PDF

Limburg Group (DC)

Pre-permian subcrob map
PDF

Upper Rotliegend Group (RO)

Depth of the base of the Upper Rotliegend Group
PDF
ARC GRID
ZMAP GRID

Thickness of the Upper Rotliegend Group
PDF
ARC GRID
ZMAP GRID

Zechstein Group (ZE)

Depth of the base of the Zechstein Group
PDF
ARC GRID
ZMAP GRID

Thickness of the Zechstein Group
PDF
ARC GRID
ZMAP GRID

Salt structures map

PDF

Lower Germanic Trias Group (RB)

Depth of the base of the Lower Germanic Trias Group

PDF
ARC GRID
ZMAP GRID

Thickness of the Lower Germanic Trias Group

PDF
ARC GRID
ZMAP GRID

PDF
ARC GRID
ZMAP GRID

PDF
ARC GRID
ZMAP GRID

Upper Germanic Trias Group (RN)

Depth of the base of the Upper Germanic Trias Group

PDF
ARC GRID
ZMAP GRID

Thickness of the Upper Germanic Trias Group

PDF
ARC GRID
ZMAP GRID

Altena Group (AT)

Depth of the base of the Altena Group

PDF
ARC GRID
ZMAP GRID

Thickness of the Altena Group

PDF
ARC GRID
ZMAP GRID

PDF
ARC GRID
ZMAP GRID

Schieland Group (SL)

PDF

ARC GRID
ZMAP GRID

Thickness of the Central Graben subgroup (SLC)

PDF
ARC GRID
ZMAP GRID

PDF
ARC GRID
ZMAP GRID

Thickness of the Scruff subgroup

PDF
ARC GRID
ZMAP GRID

Rijnland Group (KN)

Depth of the base of the Rijnland Group

PDF
ARC GRID
ZMAP GRID

Thickness of the Rijnland Group

PDF
ARC GRID
ZMAP GRID

Chalk Group (CK)

Depth of the base of the Chalk Group

PDF
ARC GRID
ZMAP GRID

Thickness of the Chalk Group

PDF
ARC GRID
ZMAP GRID

Lower and Middle North Sea groups (NL - NM)

PDF
ARC GRID
ZMAP GRID

Thickness of the Lower and Middle North Sea Groups

PDF
ARC GRID
ZMAP GRID

Upper North Sea Group (NU)

Depth of the base of the Upper North Sea Group

PDF
ARC GRID
ZMAP GRID

Petroleum Geology

Oil & gas fields map
PDF

Geothermal gradient map
PDF
ARC GRID
ZMAP GRID

Faults

Faults Zechstein and Rotliegend groups
ZMAP LINES

Faults Lower Germanic Trias Group
ZMAP LINES

Faults Upper Germanic Trias Group
ZMAP LINES

Faults Altena Group
ZMAP LINES

Faults Posidonia Shale Formation
ZMAP LINES

Faults Schieland Group
ZMAP LINES

Faults Rijnland Group
ZMAP LINES

Faults Chalk Group
ZMAP LINES

Faults Lower North Sea Group
ZMAP LINES

Faults Upper North Sea Group
ZMAP LINES

6.4 List of figures

6.5 List of tables

7 Annexes

A. Location map seismic data and wells
B. Depth maps (B1-12)
C. Thickness maps (C1-10)
D. Structural elements map
E. Fault systems and salt structures
F. Tectono-stratigraphic diagram
G. Cross sections (G1-3)
H. Biostratigraphic results (H1-2)
I. Correlation panels (I1-3)
J. Petrophysical properties (J1-20)
K. Reservoir thickness (K1-3)
L. Oil and gas fields (L1-3)
M. Measured vitrinite reflectance values (M1-3)
N. Geothermal gradient map

8 Signature

Utrecht, 1 augustus 2009

TNO Built Environment and Geosciences

J.C.. Doornenbal	J.M. Verweij	N. Witmans
Head of department	Author	Author